

FRACTURE MECHANICS OF
FIBER REINFORCED COMPOSITES

A Thesis
Presented to
the Faculty of the Department of Mechanical Engineering
University of Houston

In Partial Fulfillment
of the Requirements for the Degree
Master of Science in Mechanical Engineering

by
Leonard Douglas Power
June 1968

450456

ACKNOWLEDGMENTS

I would like to express appreciation to the following people whose assistance has made this work possible:

To the National Science Foundation for their financial support.

To my Advisor, Dr. A. C. Nunes for his invaluable suggestions and help.

To my wife, Jeannette, for her patience and understanding.

FRACTURE MECHANICS OF
FIBER REINFORCED COMPOSITES

An Abstract of a Thesis
Presented to
the Faculty of the Department of Mechanical Engineering
University of Houston

In Partial Fulfillment
of the Requirements for the Degree
Master of Science in Mechanical Engineering

by
Leonard Douglas Power
June 1968

ABSTRACT

The present investigation is a study of the stress field produced by a broken fiber in a fiber reinforced composite and the nature of failure propagation in the composite following such an initial break.

The material is simulated by a hexagonal network of elastically coupled discrete elements. Equilibrium of a typical element yields a system of first order difference equations in terms of the displacements of the elements. The displacements are then found by the method of relaxation, and stresses obtained from the resulting displacement field.

Results are given for various values of relative elastic properties and fiber volume fractions to show the effect of these parameters on stress distributions. Where applicable, results are compared to previous analyses.

A theory is offered to explain the general notch insensitivity of fiber reinforced composites based on the distribution of flaws in fibers. A recommendation for future study is included.

TABLE OF CONTENTS

ABSTRACT v

LIST OF FIGURES viii

LIST OF SYMBOLS ix

I. INTRODUCTION 1

 Description and Classification of Fiber

 Reinforced Materials 1

 The Mechanics of Fiber Strengthening 3

 Continuous Fibers 3

 Discontinuous Fibers 5

 Short Fibers--Critical Length 8

 Modes of Failure 11

 Preliminary Statement of the Problem and

 Review of the Literature 14

 Relevant Theoretical Analyses 15

 Relevant Experimental Results 19

 Limitations of Previous Studies 20

II. THE PROBLEM 23

 Method of Solution 23

 Analysis of the Model 25

III. RESULTS 31

IV. CONCLUSIONS 46

V. RECOMMENDATIONS FOR FURTHER RESEARCH	48
REFERENCES	50
APPENDIX I	52
APPENDIX II	55
APPENDIX III	58
APPENDIX IV	70

LIST OF FIGURES

FIGURE		PAGE
1.	Illustration of Stress Distribution for Three Possible Conditions.....	7
2.	Schematic Representation of the Interaction Between Fiber and Matrix for a Short Fiber Which is Longer than Critical Length.....	9
3.	Schematic Representation of the Role of Critical Fiber Length in a Composite...	10
4.	Possible Fracture Types.....	13
5.	Equivalent Model of Fiber Reinforced Composite.....	24
6.	Idealized Model of Fiber Reinforced Composite as a Network of Hexagonal Unit Cells.....	26
7.	A Typical Element.....	27
8.	Shear Reaction Between Corresponding Elements in Adjacent Fibers.....	30
9,10	Interface Shear Stress Along Broken Fiber, Comparing Results From Relaxation Method to Results Based on Cox's Theory.....	33
11,12	Tensile Stress in Broken Fiber Comparing Results From Relaxation Method to Results Based on Cox's Theory	35
13,14,15	Interface Shear Stress Near the End of a Broken Fiber.....	37
16,17,18	Distribution of Fiber Stress Along a Broken Fiber.....	40
19,20,21	Perturbation of Stress in Fiber Immediately Adjacent to Break.....	43

LIST OF SYMBOLS

σ	Tensile Stress
τ	Shear Stress
$\sigma_{f\infty}$	Tensile Stress in a Continuous Filament
τ_i	Interface Shear Stress
γ	Shear Strain
$\bar{\gamma}$	Mean Shear Strain
x	Distance From Plane of Fiber Break
u	Displacement in the x -Direction
d_f	Fiber Diameter
V_f	Fiber Volume Fraction
t	Distance Between Fibers
\bar{t}	Mean Distance Between Fibers
E	Modulus of Elasticity
G	Shear Modulus
f, m, c	Subscripts Applying to Fiber, Matrix, and Composite, Respectively.

CHAPTER I

INTRODUCTION

There has recently been increasing interest in the development of fiber reinforced composite materials for structural applications. Such composites are formed by imbedding parallel bundles of strong fibers with large elastic moduli in a more ductile, low modulus binder which serves to join them together, protect them from adventitious damage, and allow load transfer to the fibers. The principles of fiber reinforcement have been understood in a general way for many years and have been extensively exploited in the production of commercial fiberglass.

I. DESCRIPTION AND CLASSIFICATION OF FIBER REINFORCED COMPOSITES

Interest in such composite materials began with the development of glass fiber reinforced plastics in the early 1940's. The first fiberglass was made by soaking a woven glass fiber mesh in a thermosetting polymer and allowing it to harden in the desired shape. Laminated composites were made by stacking several such sheets and allowing them to set under pressure. This type of laminate is still in wide use. In the intervening years, many improvements have been

made both in the constituent materials and the fabricating techniques.

The confirmation of the high strength of short fibers or "Whiskers" by Brenner^{1*} in 1956 and the discovery by McDanel, Jech and Weeton² that the properties of fiber reinforced composites were essentially the same for continuous and discontinuous fibers led to the conclusion that very high strength materials might be produced by whisker reinforcement of metals. The mechanical properties of some reinforcing filaments and whiskers are tabulated in Appendix I. Significant progress has recently been made in the technology of whisker-strengthened metals, although the laboratory techniques used have not been applied on a commercial scale.

Fiber reinforced composites may be classified according to the relative lengths of the fibers used or the manner in which they are oriented within the composite. In the metals, common reinforcing elements are whiskers, which are discontinuous due to manufacturing limitations rather than design, and are generally oriented, as nearly as possible, parallel to the direction of principal stress. Short fibers also find wide application as fillers in molded plastic products. These consist of chopped organic fibers which are mixed into

*Superscripts refer to references an end of thesis.

polymers before molding to add rigidity and dimensional stability. Their orientation within the material is essentially random.

When the reinforcing fibers are easily produced in continuous strands, as with glass or steel filaments, the location and orientation of the filaments may be controlled so as to obtain the maximum benefit of composite strengthening for the particular application. This type of fabrication is applied in the manufacture of filament-wound tubing and pressure vessels. When filament-winding is not applicable, a degree of selective orientation may still be achieved by the use of fiber cloth.

II. THE MECHANICS OF FIBER STRENGTHENING

Continuous Fibers

In order to use the high strength of reinforcing filaments in a composite, the filaments must be oriented so that the worst load carried by the material will be applied parallel to the fiber axes. When a composite containing continuous filaments is loaded parallel to the direction of the fibers, the fibers and matrix may be expected to undergo essentially equal strain, which leads to a simple "Law of Mixtures" determination of the mechanical properties of the composite in terms of the properties of the constituents.

These principles are developed in Appendix II. With this assumption of equal strain, it is convenient to consider the behavior of such a composite in terms of strain rather than stress. If the filaments and the matrix are elastic, the composite will behave elastically according to the Law of Mixtures.

When a certain value of strain is exceeded, the composite will deviate from elastic behavior and deformation processes that will ultimately result in fracture will be initiated in the composite. Four things may produce such deviation: (1) yielding of the reinforcing fibers, (2) yielding of the matrix, (3) fracture of the matrix, or (4) fracture of the reinforcing fibers. The first of these is unlikely since commercially used fibers are highly brittle. The second is of little interest in terms of fracture, although it does produce a change in the over-all elastic modulus of the composite, an effect which was noted by Kelly and Tyson³. The great ductility of the common matrix materials precludes the third unless there are voids or notches in the matrix. Consequently, tensile fracture of the fibers is the most likely mechanism by which failure is initiated.

When a fiber has broken, a discontinuity is introduced which significantly affects the behavior of the composite

which then enters the discontinuous stage prior to ultimate fracture.

Discontinuous Fibers

If a composite contains discontinuous fibers, as would be the case if a composite made with continuous filaments had been strained sufficiently to break some of the filaments, or if the composite were made with discontinuous fibers (or whiskers) aligned in the direction of principal stress, the load must be transmitted from one fiber to another through the matrix. When the composite is stressed in the direction of fiber alignment the axial displacement of the two components will be different due to the difference in their elastic moduli and shear stresses will be produced in the direction of the fiber axes⁴. These shear stresses are the mechanism by which load is transferred from the matrix to the fibers. Any study of mechanical properties or fracture mechanics of fiber reinforced composites must be centered around the nature of this load transfer mechanism and the associated stress distribution, especially in the vicinity of a fiber end.

The distributions of shear and tensile stresses are illustrated schematically in Figure 1 for three possible conditions. When the matrix deforms elastically only, the

shear stress is a maximum in the vicinity of the fiber end, then drops sharply, approaching zero asymptotically as the fiber tensile stress approaches a value $\sigma_{f\infty}$, which is the stress of an infinitely long fiber under the same loading conditions. When the matrix or interface yields, the interfacial shear again rises to a maximum near the fiber end, but distributes itself over a much greater portion of the fiber surface, so transfer of the same load from the matrix to the fiber now requires a greater fiber length. It is also possible, in a discontinuous composite where fiber strains may differ, that the fracture strength of the interface bond may be exceeded before the matrix yield stress is reached. Such a condition is especially likely to be encountered in glass fiber reinforced polymers. In this case, a shear failure will occur at the fiber-matrix interface and a separation of fiber and matrix will start at the fiber end and propagate along the length of the fiber. In the region of such a separation, the fiber-matrix interaction may be considered to be frictional. Outwater⁵ assumes that frictional forces in glass fiber reinforced polymers are proportional to contact stresses between fiber and matrix, and derives expressions for their magnitudes.

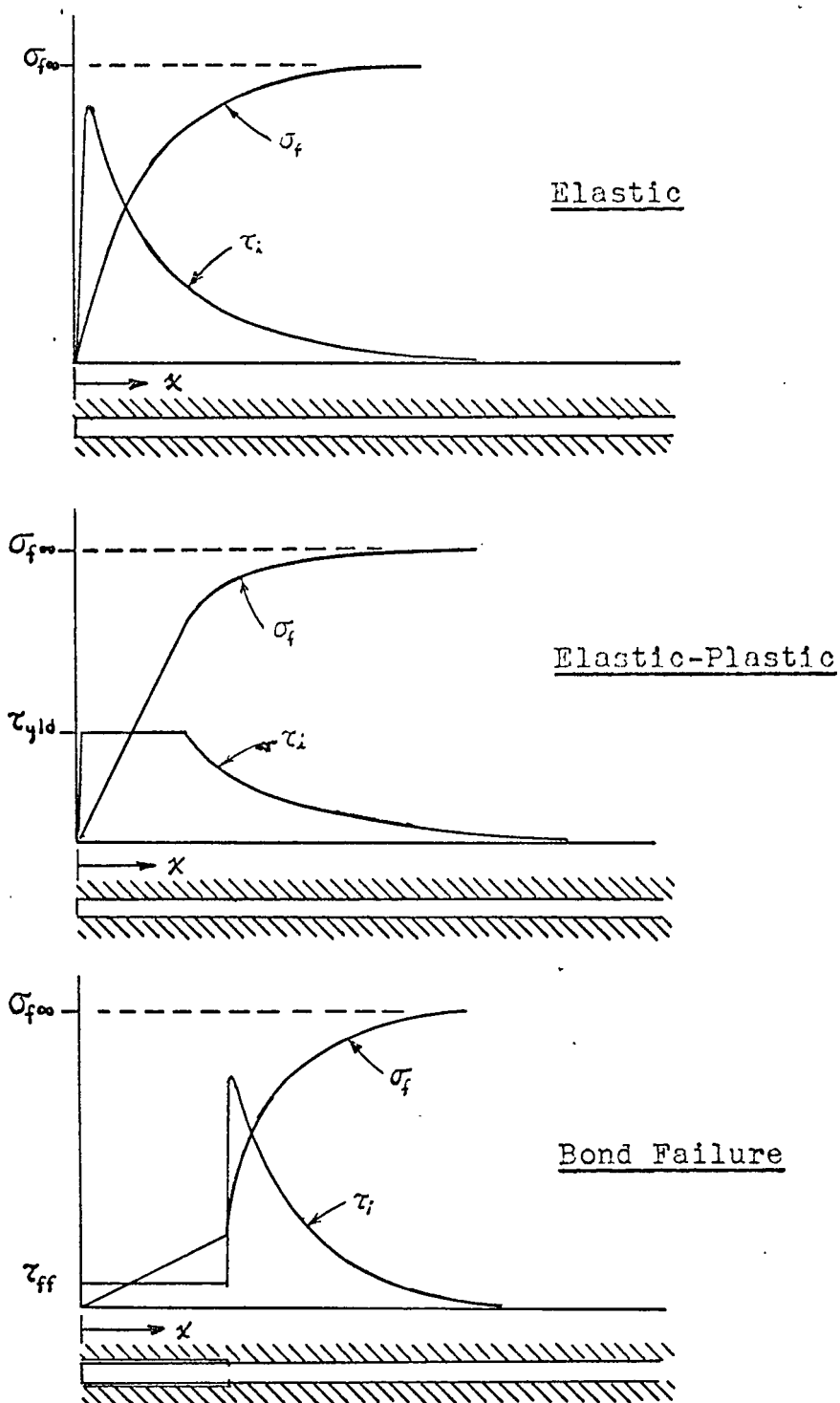


Figure 1. Illustration of stress distribution for three possible cases.

Short Fibers--Critical Length

The distribution of shear and tensile stresses in the vicinity of a short fiber will be similar to that of a semi-infinite fiber; the principal exception being that symmetry requires that the interface shear be zero at the mid-point of the fiber. Schematically represented in Figure 2 are the distributions of interface shear and fiber tension in the vicinity of a short fiber imbedded in a weaker matrix, assuming that the integrity of the bond is maintained. As was seen in the case of the semi-infinite fiber (Figure 1), when the matrix deforms elastically only, the shear stress builds up to a maximum value which approaches that of an infinitely long fiber where end effects are negligible. When the matrix or interface yields, the interface shear again rises rapidly near the fiber end, but distributes itself over a much greater portion of the fiber so transfer of the same load to the fiber now requires a greater fiber length. The minimum fiber length required to reach a maximum tensile stress that is 97 percent of $\sigma_{f\infty}$ is called the critical transfer length, L_c . A short L_c is indicative of efficient stress transfer between matrix and fiber⁶. When the fiber length is less than the critical length, the load carrying capacity of the fiber is low, and its value as reinforcement is reduced. This is illustrated in Figure 3.

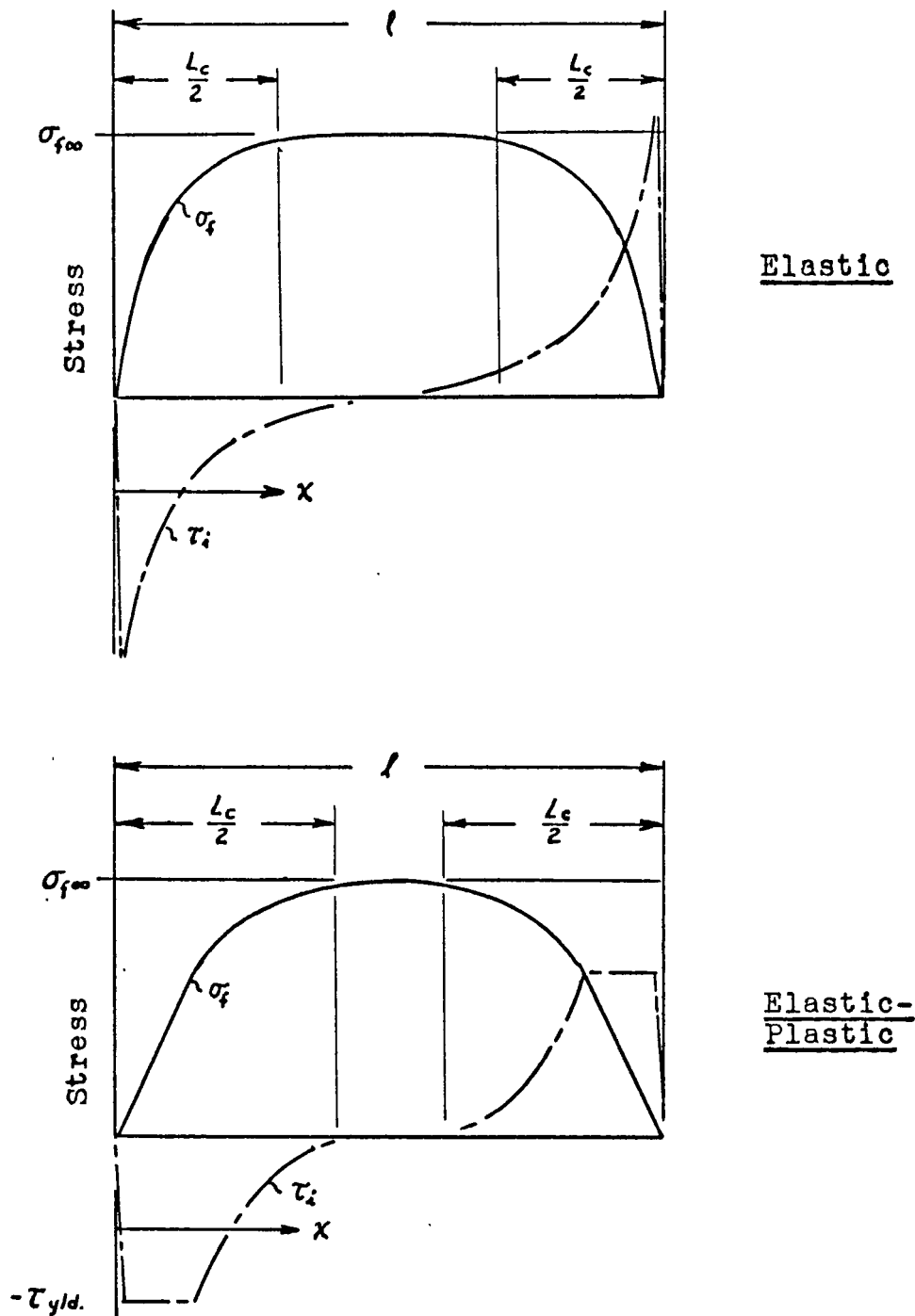


Figure 2. Schematic representation of the interaction between fiber and matrix for a short fiber which is longer than critical length.

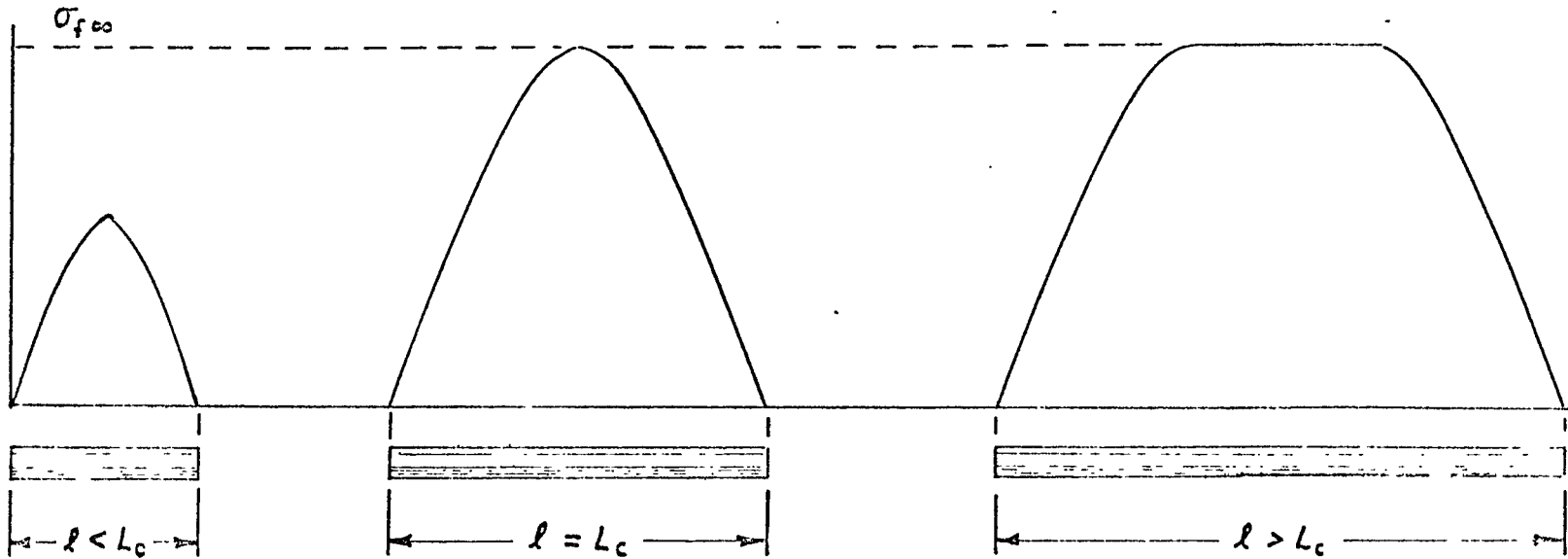


Figure 3. Schematic illustration of the role of critical fiber length in a composite.

Modes of Failure

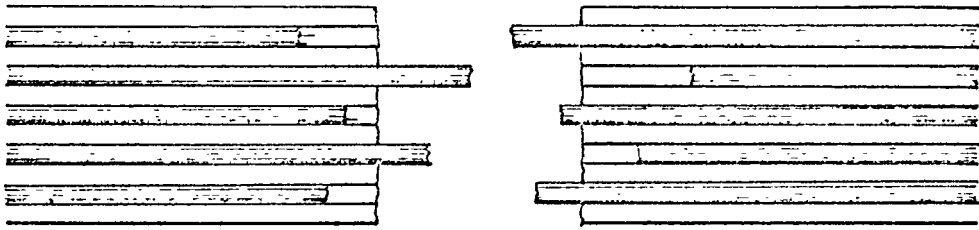
This study will treat the mechanics of tensile failure of a fibrous composite subsequent to an initial fiber fracture. Brittle fibers have a distribution of flaws or imperfections which result in fiber fracture at various stress levels⁷, and it has already been pointed out that the fracture process is most likely to begin with a fiber fracture. When such a break occurs, several possibilities for the future behavior of the composite exist.

First, the high interface shear stresses could produce interface failure propagating away from the break along the fiber. Such an interface failure separates the fiber from the matrix over the length of the bond failure and renders that portion of the fiber ineffective as a load-carrying element, but results in no appreciable stress concentration around the fiber break. The load that had previously been carried by the broken fiber is now distributed among the remaining fibers. As the stress increases, more fibers break and a given cross-section is penetrated by an increasing number of ineffective fibers. Total composite failure occurs when the load on a particular cross-section exceeds the capacity of the remaining effective fibers intersecting it. At this point the matrix and the remaining fibers fracture.

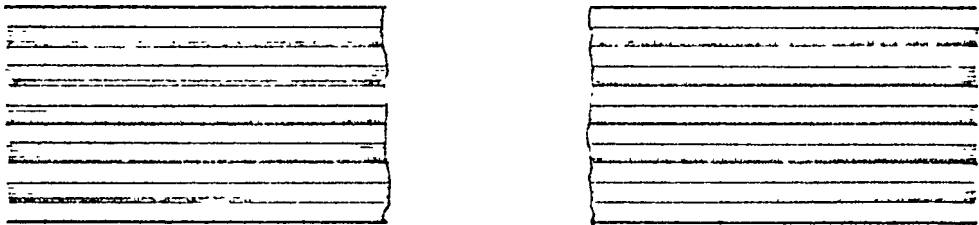
The resulting fracture surface contains alternating holes and protruding fibers as illustrated in Figure 4. This type of composite failure is common to fiber reinforced polymers⁵ and is usually called a "pull-out" failure.

Second, a fiber break may produce high local stresses that extend to the adjacent fiber, which breaks as a result of the stress concentration. If the composite is subject to this type of transverse fracture propagation, the composite will exhibit a sudden, brittle type failure (or quasi-brittle if the matrix is very ductile). The fracture surface is illustrated in Figure 4.

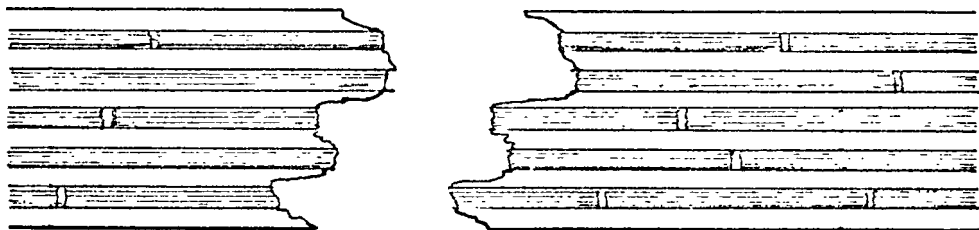
A third possibility, to be elaborated more fully later, is that the localized nature of the stresses around a fiber break, together with the nature of the flaw distributions in the adjacent fibers may be combined in such a way that failure will be arrested at the interface of the adjacent fibers. This crack-arresting property of composite structures accounts for much of their toughness, and Cooper and Kelly⁸ have shown that notch-insensitive composites can even be made with constituents that are individually notch-sensitive. If a composite resists crack propagation either along the interface, or transverse to adjacent fibers, it will be possible to increase the load, while subsequent breaks occur at other points of fiber weakness independent of the previous



Pull-Out



Brittle



Tough

Figure 4. Possible fracture types.

break. Increasing the load will then produce an increasing number of randomly located fiber fractures until a sufficient number of fractures accumulate near some cross section to produce a weak surface. At the point of incipient failure, all the previously mentioned failure modes may interact to produce the final fracture. These progressive stages of fracture were confirmed by Rosen⁷ who observed initial fiber fractures in a glass-epoxy specimen at less than 50 percent of the ultimate load.

Since the fiber stress rises sharply at the end, approaching $\sigma_{f\infty}$ asymptotically, it is likely that at a distance sufficiently removed from a break, a broken fiber may break again. This behavior has been confirmed by Rosen⁷, who counted more fractures than fibers in a failing model. When this happens, the composite contains fibers of finite length. The following section outlines past theoretical analyses of stresses around a fiber of finite length within a reinforced composite material which undergoes a stress parallel to the direction of the fibers.

III. PRELIMINARY STATEMENT OF THE PROBLEM AND REVIEW OF THE LITERATURE

It was the purpose of this study to treat the initiation of fracture in a strongly bonded fiber reinforced composite

by devising an elastic "equivalent model" of such a composite with one broken fiber and solving for the stresses in the model by the method of relaxation.

Relevant Theoretical Analyses

If a composite contains only continuous filaments, the load is applied directly to them so that the stress is constant over the length of the fiber, and there is no shear at the fiber-matrix interface. In such a case the proportion of the applied load carried by the fibers can be calculated from the "law of mixtures" derived in Appendix II. If, however, a composite contains discontinuous or short fibers, an analysis of the stresses is much more involved, and an exact solution does not seem possible at this time. However, five approximate theories based on a cylindrically symmetric model have been presented and are summarized below in chronological order. Details of the derivations are presented in Appendix III.

In 1952, H. L. Cox⁴ presented a theory for the case of an elastic fiber in a completely elastic matrix, assuming a perfect bond between fiber and matrix, equal lateral stiffness of fiber and matrix, and negligible load transfer through the end of the fiber. To obtain expressions for stress distribution, he assumed that the matrix is strained

homogeneously, but the stress and strain is locally perturbed by the transfer of load to the more rigid fibers. This perturbation is assumed to be governed by the equation:

$$\frac{dP}{dx} = H(u-v) \quad (1)$$

where x is the distance from the fiber end, P is the local load carried by the fiber, u is the local displacement, v is the displacement the same point would have if the fiber were not present, and H is a constant*. Solution of the above differential equation with boundary conditions yields:

$$\sigma_f = \frac{(E_f - E_m)\sigma_a}{E_m} \left[1 - \frac{\cosh\beta\left(\frac{l}{2} - x\right)}{\cosh\beta\frac{l}{2}} \right] \quad (2)$$

$$\tau_i = \frac{(E_f - E_m)\sigma_a}{E_m} \frac{d_f}{4} \beta \frac{\sinh\beta\left(\frac{l}{2} - x\right)}{\cosh\beta\frac{l}{2}} \quad (3)$$

In 1956, J. Ogden Outwater, Jr.⁵ presented a theory for the specific case of reinforced plastics. Since the bond strength in plastics is low, he assumed that the interaction between fiber and matrix was through friction at the interface. He further assumed that load is carried entirely by the fibers, and that the fibers are connected to the matrix material by a thin film of matrix material whose thickness

*See Appendix III for definitions of constants in this section.

is negligible compared to the other dimensions of the system and thus does not deflect in shear. The friction at the fiber-matrix interface is assumed to arise from the shrinkage of the matrix onto the fiber during production. The thin film of matrix material is then treated as a thin cylinder with hoop stress equal to the yield stress of the plastic. The result is a constant shear stress and a linear fiber stress distribution:

$$\sigma_f = \frac{\mu \sigma_y x}{r_f^2} \quad (4)$$

up to a distance x_0 from the end, given by

$$x_0 = \frac{E_f \epsilon r_f^2}{\mu \sigma_y t} \quad (5)$$

and for $x > x_0$,

$$\sigma_f = \sigma_{f\infty} = E_f \epsilon \quad (6)$$

In 1963, N. F. Dow⁹ presented a theory for the case of an elastic fiber in a completely elastic matrix with perfect bonding between fiber and matrix. The load was assumed applied at one end to the matrix alone. At the other end, both fiber and matrix were assumed loaded so that the strain in each was the same, simulating the midplane of a symmetrically loaded short fiber. It was further assumed that the matrix deformed in such a way that straight radial lines

remained straight as the matrix deformed in shear. These assumptions yield, for the shear at the interface:

$$\tau_i = \frac{\lambda P_m \sinh \left[\frac{\lambda}{d_f} \left(\frac{l}{2} - x \right) \right]}{4 \left(A_f + \frac{A_m E_m}{E_f} \right) \cosh \frac{\lambda l}{2d_f}} \quad (7)$$

and for the tensile stress in the fiber:

$$\sigma_f = \frac{P_m}{A_f + \frac{A_m E_m}{E_f}} \left[1 - \frac{\cosh \frac{\lambda}{d_f} \left(\frac{l}{2} - x \right)}{\cosh \frac{\lambda l}{2d_f}} \right] \quad (8)$$

In 1964, B. Walter Rosen⁷ produced a modification of Dow's theory. Rosen's model differs from Dow's in that Rosen considers the fiber to be surrounded by a matrix which in turn is surrounded by a material having the average properties of the composite. In Rosen's model, he assumes perfect bonding at the fiber-matrix interface, no load transferred through the ends of the fiber, and that the fiber and average material carry only tensile stresses, while the matrix material carries only shear stresses. With these assumptions, an equilibrium equation is solved to obtain:

$$\tau_i = \frac{2 G_m \sigma_c d_a^2 \sinh \eta \left(\frac{l}{2} - x \right)}{\eta E_a (d_a - d_f) (d_a^2 - d_m^2) \cosh \eta \frac{l}{2}} \quad (9)$$

and,

$$\sigma_f = \frac{\sigma_c d_a^2 E_f}{E_a (d_a^2 - d_m^2) + E_f d_f^2} \left[1 - \frac{\cosh \eta \left(\frac{l}{2} - x \right)}{\cosh \eta \frac{l}{2}} \right] \quad (10)$$

In 1965, Kelly and Tyson³ produced an analysis for the case of the matrix in the plastic state. They assume that the whole of the matrix yields plastically and flows past the fiber which is stretched by the shear acting at the interface. Applying the Tresca yield criterion, this interface shear stress is the yield stress in shear of the matrix and is a constant. The equilibrium equation for the fiber integrates to give:

$$\sigma_f = \frac{2 \tau_y \left(\frac{l}{2} - x \right)}{r_f} \quad (11)$$

Relevant Experimental Results

In 1965, Tyson and Davies¹⁰ carried out photoelastic experiments on a two-dimensional model and compared the results to the theories of Cox and Dow. Their results indicate reasonable agreement at a distance more than one fiber diameter from the end, but the interface shear was found to be more than twice that predicted by the theories at points very near the ends. Also in 1965, Schuster and Scala¹¹ carried out photoelastic studies on a three-dimensional model and compared the results to Dow's theory. Their results indicate reasonable agreement with the theory at distances of more than two fiber diameters from the ends of the fiber. At points near the ends, they measured interface shears which

were higher than those predicted by theory, although the discrepancy was not nearly so pronounced as in the experiments of Tyson and Davies.

Limitations of Previous Studies

In the three theories which use a model consisting of an elastic fiber in an elastic matrix (Cox, Dow, and Rosen), the results are similar in form. The stresses are in all cases expressed in terms of hyperbolic functions of x , the only differences being in the coefficients involved. The theoretical results from the three analyses are generally in closer agreement with each other than with experimental evidence, so that there is no experimental justification for favoring one particular analysis above the others. These theories have been applied to the problem of determining the elastic properties of fibrous composites containing discontinuous fibers, and have produced reasonable results⁷. The fact that the photoelastic measurements of interface shear mentioned in the preceding section indicated much higher values than were predicted by the theories would cast some doubt on the theories. However, it should be noted that approximations are involved in both the theoretical and experimental models. The fact that the theoretical and experimental results agree well at points more than four fiber diameters from the end suggests that the discrepancy is

related to end conditions such as (1) load transfer and/or (2) stress concentration factor at the fiber ends. The first effect was considered by Tyson and Davies¹⁰ who found that interface shear was increased by end bonding. The second effect was considered by Schuster and Scala¹¹ who confirmed the existence of a high stress concentration effect for a blunt ended fiber.

The "friction" model does not actually apply to the case being considered, but is mentioned since it is so closely related to the above three. It might have some application to pull-out failure of weakly bonded composites.

The theoretical model proposed by Kelly and Tyson was accompanied by extensive experimental work on their part which tended to confirm the plastic matrix failure mechanism.

A shortcoming which all the theories have in common is the assumption of cylindrical symmetry around the fiber in question. This assumption always involves the radial distance from the fiber-matrix interface to another such interface. Since this varies with direction, some sort of average must be used. This yields an average shear stress, while the maximum may be of more interest in terms of failure.

Another significant limitation is that while all the theories treat the effect of a fiber fracture on the fiber

itself, they are not adaptable to an estimate of the influence of a fiber fracture on the stresses in adjacent fibers.

CHAPTER II

THE PROBLEM

It was the purpose of this study to estimate the fiber tensile stresses and interface shear stresses resulting from a fiber break in a strongly bonded composite subjected to a stress parallel to the reinforcing fibers.

I. METHOD OF SOLUTION

For the purpose of analysis, the material is approximated by the discrete model shown in Figure 5. In the model, each element is connected along the axis of the fiber through an elastic coupling characterized by a tension spring constant, K_T . It is also connected to a corresponding element in an adjacent fiber through an elastic coupling characterized by a shear spring constant, K_S . A fiber break is then simulated by a broken tension spring.

Equilibrium conditions require that the net force acting on any element of the model be zero. If the spring constants are known, the net force, F_{ij} , acting on the (i,j) element can be treated as a discrepancy, or residual at that point and is expressible as a first-order difference equation in terms of the displacements, u_{ij} . This is sufficient to set up a numerical solution for the displacement field by the

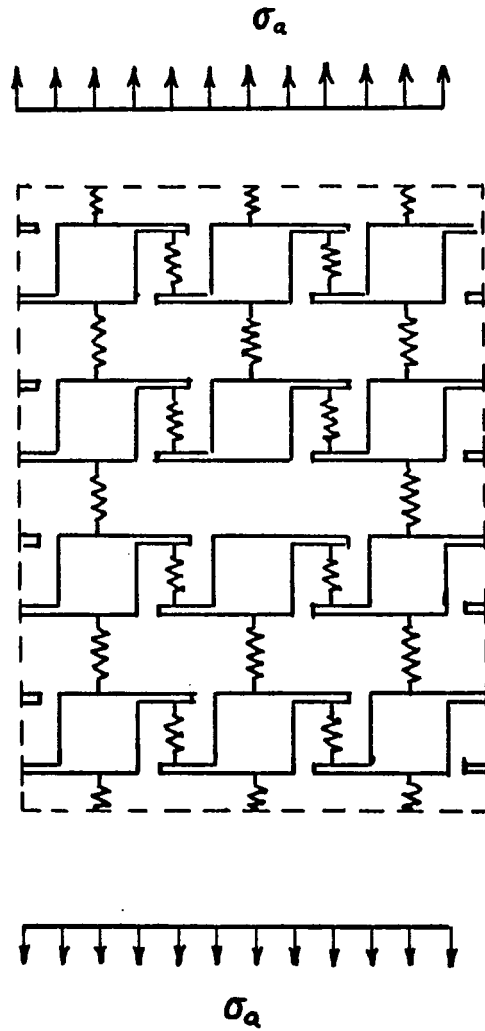


Figure 5. Equivalent Model of a fiber-reinforced composite.

method of relaxation.¹⁵ The procedure used is described in the following paragraph.

First, an initial displacement field was assumed. The displacement field which would result if there were no missing spring is an easily calculated, reasonable first assumption, and was used in this study. With these starting values, an iterative procedure was instituted as follows:

1. Find the largest $|F_{ij}|$.
2. Correct $u_{i,j}$ so that $F_{ij} = 0$.
3. Repeat until the maximum $|F_{ij}|$ is less than some predetermined limit.

II. ANALYSIS OF THE MODEL

For this analysis, a fiber reinforced composite is assumed to have the fibers arranged in a hexagonal pattern, as shown in Figure 6. The model is taken to be composed of "unit cells", each of which consists of a fiber with the matrix material included in the hexagonal region associated with that fiber. A length Δx of such a "unit cell" is then taken as the typical composite element. The element is shown in Figure 7.

Each element is elastically coupled to its eight adjacent elements. The coupling between adjacent elements within

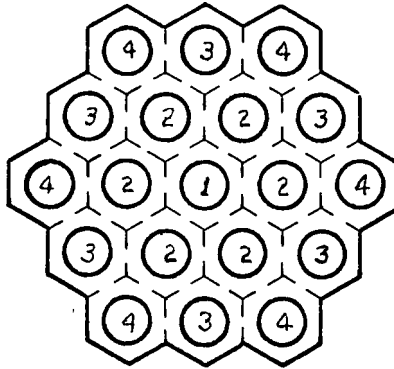
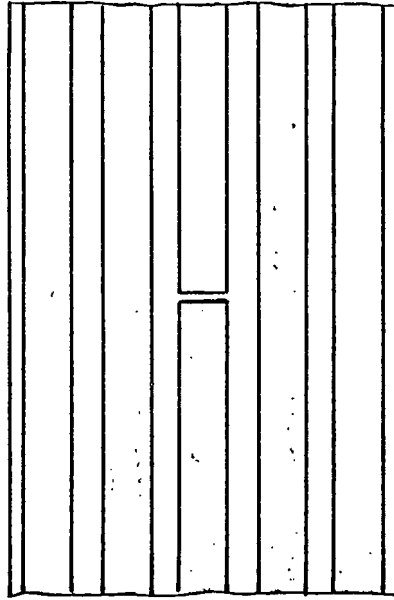


Figure 6. Idealized model of a fiber reinforced composite as a network of hexagonal unit cells.

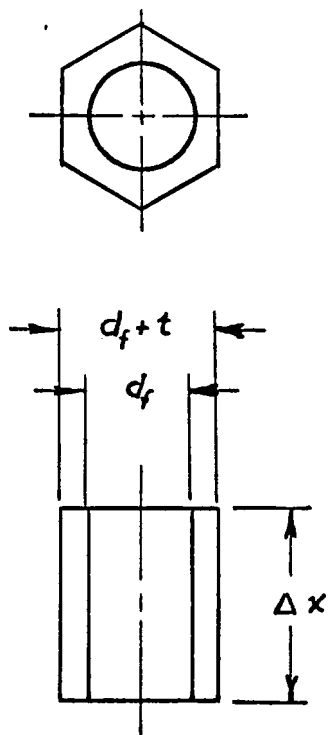


Figure 7. A typical element.

the same cell is characterized by a "tension spring constant," K_T , and the coupling between corresponding elements in adjacent cells is characterized by a "shear spring constant," K_S .

To evaluate K_T , consider two adjacent points within the j^{th} unit cell, (i, j) and $(i+1, j)$. These points are a distance Δx apart, so the "tension spring" connecting them is the elastic element shown in Figure 7. If $u_{i,j}$ and $u_{i+1,j}$ are the respective displacements, then the tensile force in this elastic element is given by:

$$F = \sigma_f A_f + \sigma_m A_m = K_T (u_{i+1,j} - u_{i,j}) \quad (12)$$

Since the thickness of the matrix layer in most composites is thin compared to the fiber diameter and E_m is small compared to E_f , we can assume, with small error, that the strain in the fiber is equal to the strain in the matrix. Also assuming that both fiber and matrix are linearly elastic,

$$\sigma_f = E_f \epsilon \quad \text{AND} \quad \sigma_m = E_m \epsilon \quad (13)$$

Strain and displacements are related by:

$$\epsilon = \frac{\Delta u}{\Delta x} = \frac{u_{i+1,j} - u_{i,j}}{\Delta x} \quad (14)$$

then substituting equations (13) and (14) into (12):

$$K_T = \frac{A_f E_f + A_m E_m}{\Delta x} \quad (15)$$

To evaluate K_s , consider the influence of the $(i, j+1)$ element on the (i, j) element (Figure 8). If u_{ij} and $u_{i,j+1}$ are not equal, there is a shear force acting on the interface between the two elements is given by:

$$F = K_s (u_{i,j+1} - u_{i,j}) = G_m \bar{\gamma} A_i \quad (16)$$

where $\bar{\gamma}$ is an average shear strain at the cell interface.

Since for most composites $G_f \gg G_m$ it is assumed that the shear strain in the fiber material is negligible, and:

$$\bar{\gamma} = \frac{u_{i,j+1} - u_{i,j}}{\bar{x}} \quad (17)$$

where \bar{x} is the mean distance between the fibers normal to the cell interface. Then substituting equation (17) into (16) and solving for K_s , we have:

$$K_s = \frac{G_m A_i}{\bar{x}} \quad (18)$$

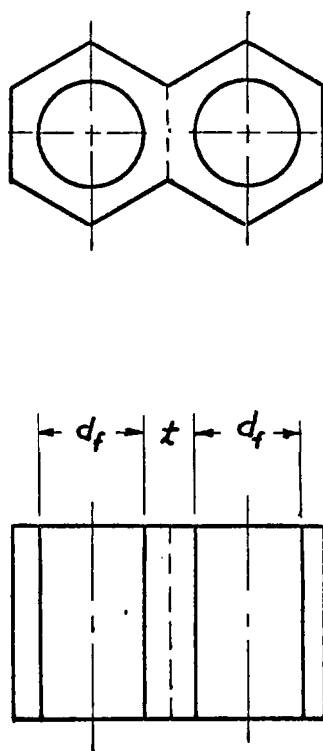


Figure 8. Shear reaction between corresponding elements in adjacent fibers.

CHAPTER III

RESULTS

Numerical calculations were made on the model described in Chapter II using typical elastic constants for three different fiber-matrix combinations, and varying volume fractions for each case.

Interface shear stresses and tensile stresses along the broken fiber are compared with values obtained from Cox's model in Figures 9 through 12. It should be noted that in the discrete model the shear stress varies around the fiber due to the variation of interface distance with direction. In the relaxation procedure, an average shear was used to determine equilibrium of fiber segments, while the maximum is displayed in the result. Cox's model only gives the average shear, the maximum shear being somewhat larger. The disagreement with Cox seen in Figure 11 is typical of low volume fractions, irrespective of elastic properties. The discrete model may be expected to be better than Cox's model at high volume fractions. The crossover of shear stresses in Figure 11 might indicate breakdown at volume fractions below about 0.75, but a proper choice of parameters in Cox's model is difficult at high volume fractions, and the error may lie in the Cox theory here.

The effect of volume fraction on the stress distribution is illustrated in Figures 13 through 18.

The effect of a fiber break on the tensile stresses in the adjacent fiber (fiber 2, Figure 6) is shown in Figures 19 through 21. Although the relaxation procedure was continued until the residuals were less than 0.5 percent of the total fiber load, the fiber break produced no perturbation of tensile stress in fibers beyond the ones immediately adjacent to the broken fiber.

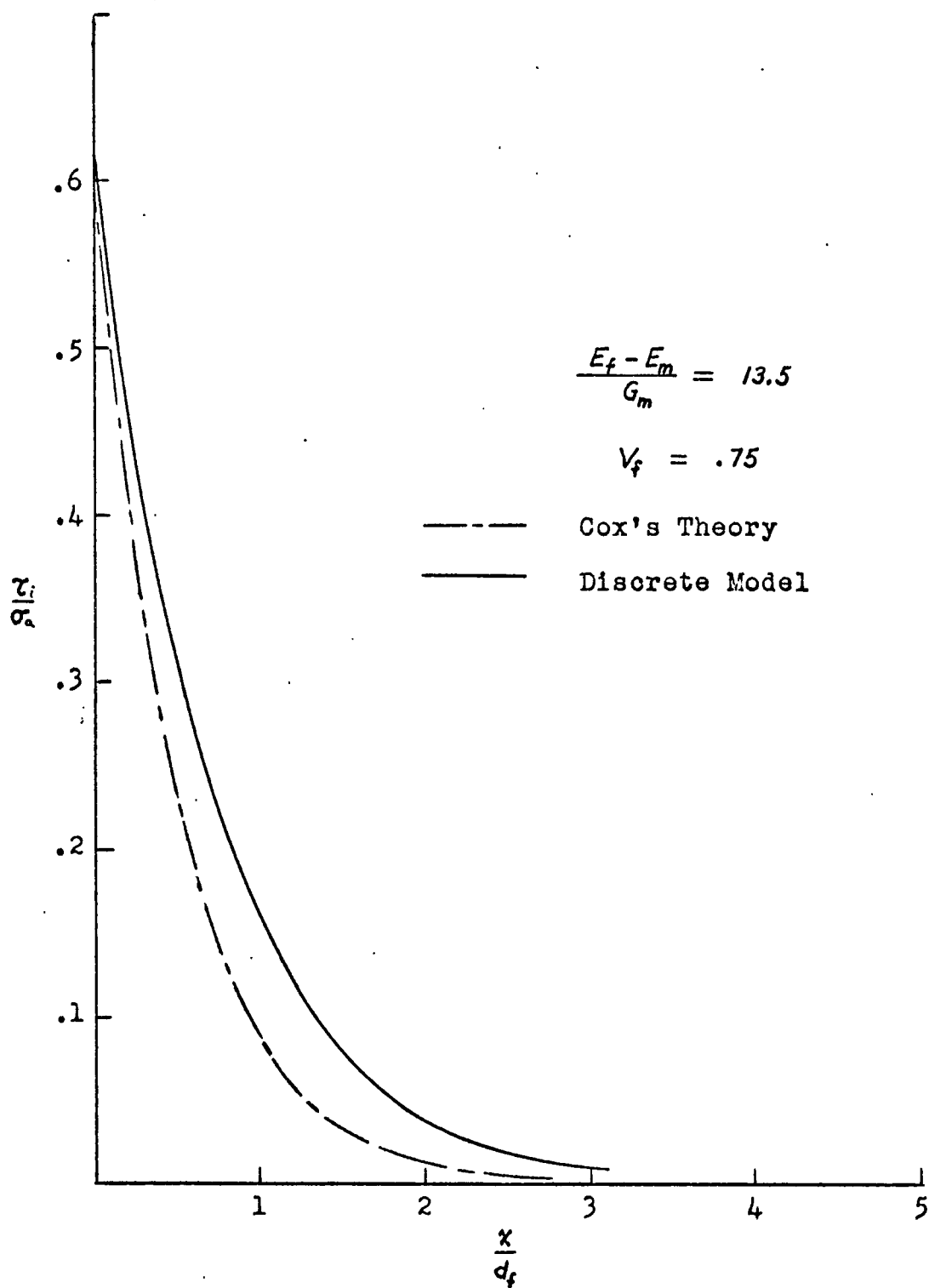


Figure 9. Interface shear stress along a broken fiber, comparing results from relaxation method to results based on Cox's theory.

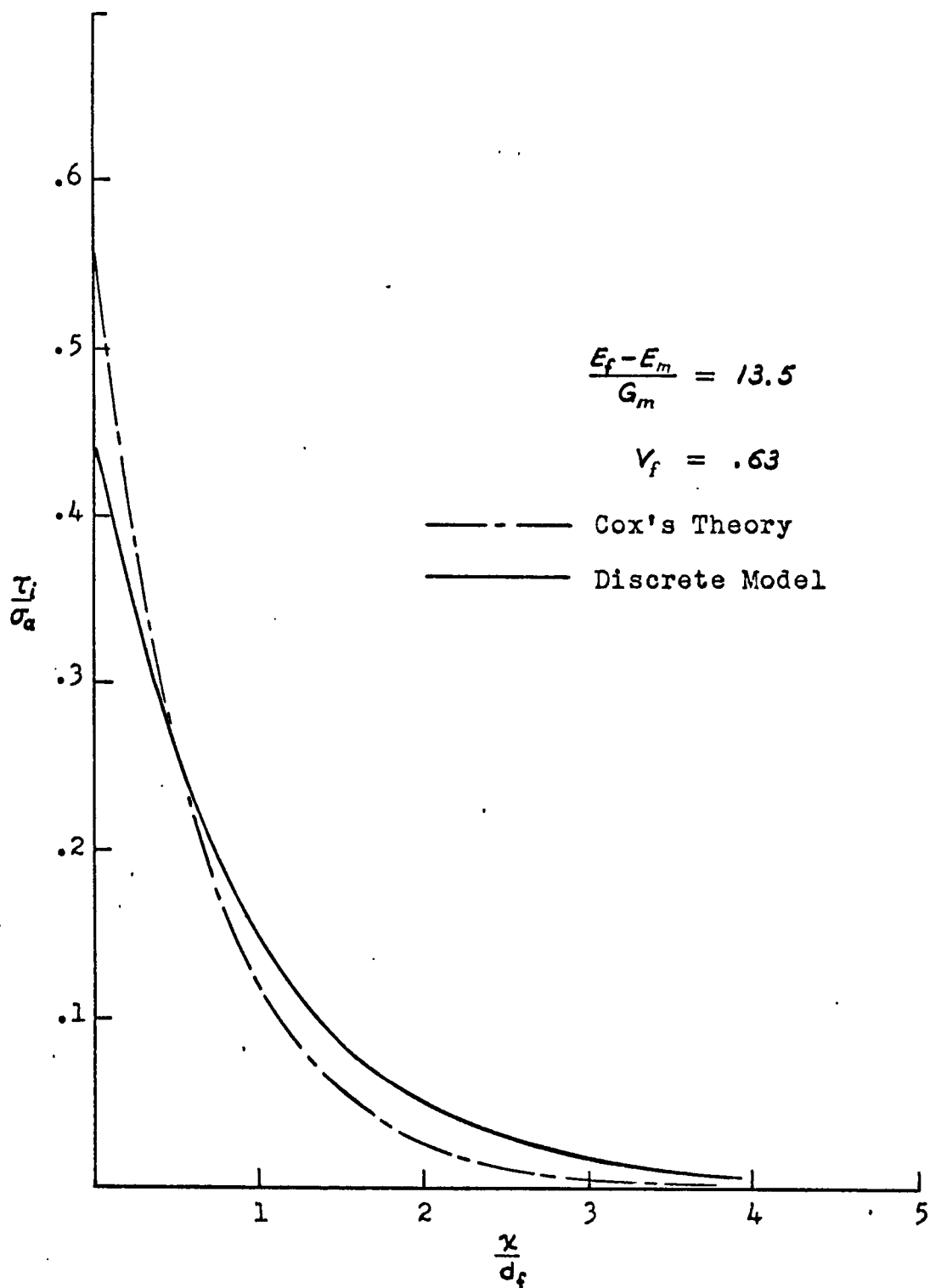


Figure 10. Interface shear stress along a broken fiber, comparing results from relaxation method to results based on Cox's theory.

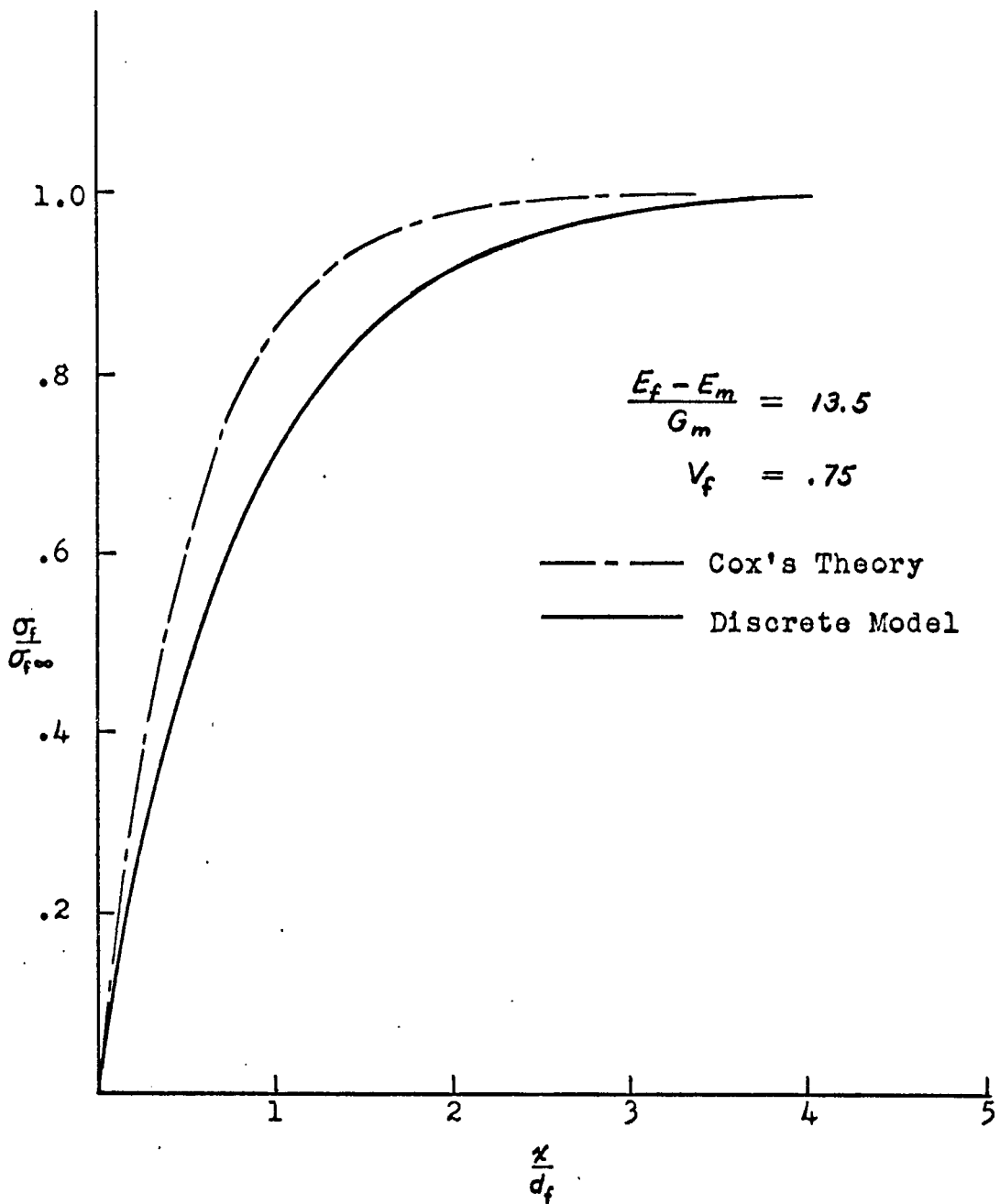


Figure 11. Tensile stress in a broken fiber, comparing results from relaxation method to results based on Cox's Theory.

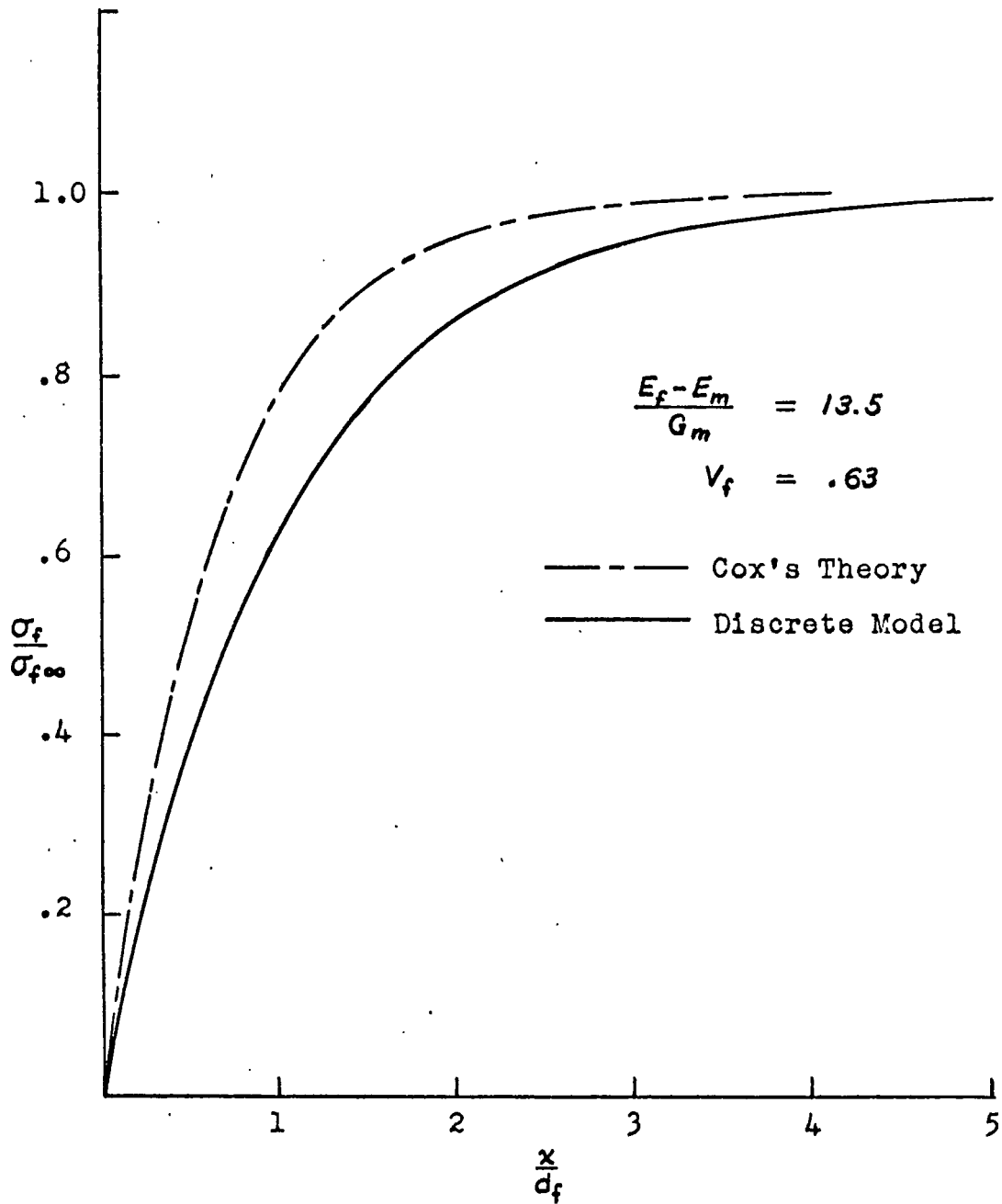


Figure 12. Tensile stresses in a broken fiber, comparing results from relaxation method to results based on Cox's Theory.

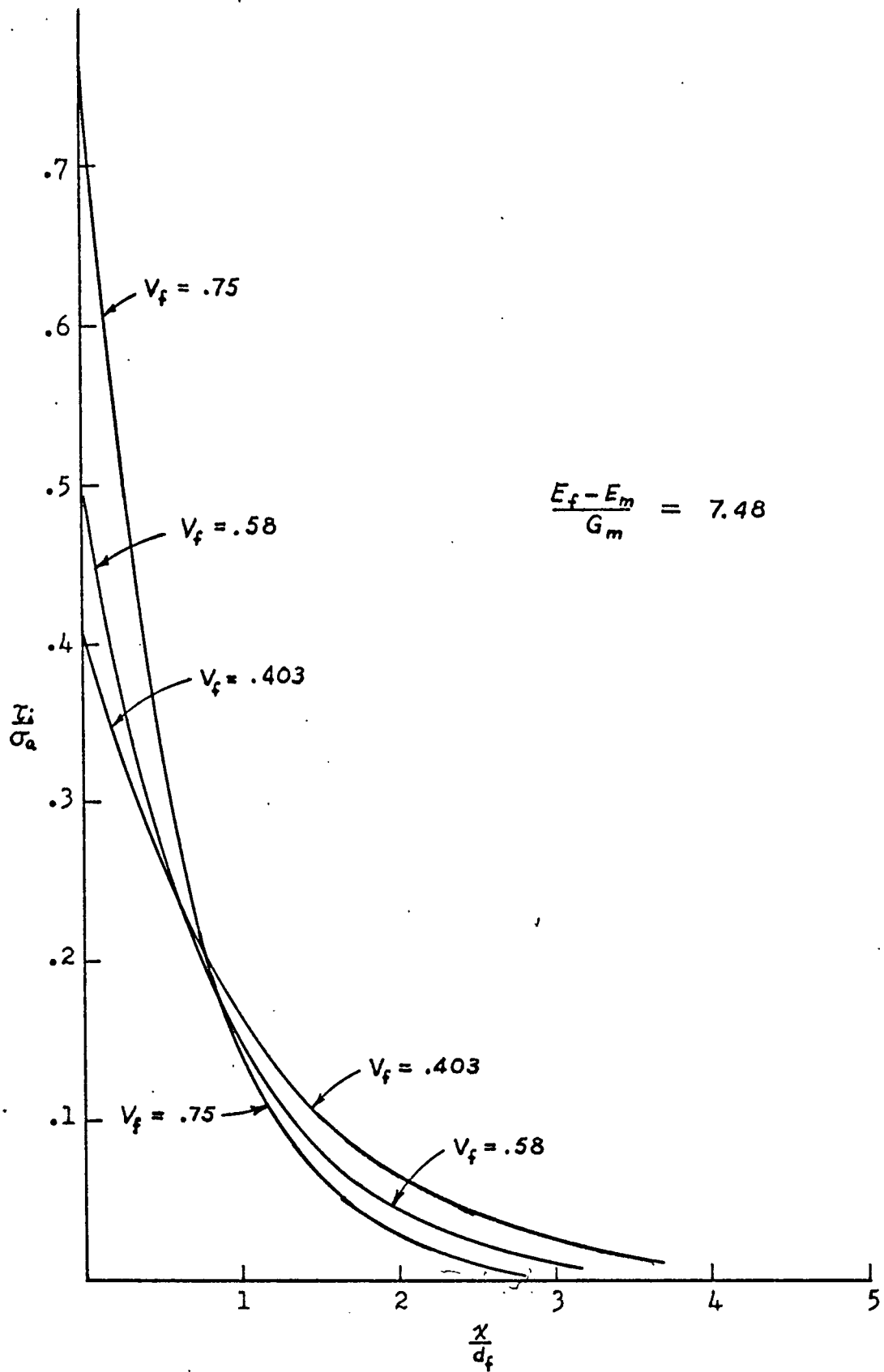


Figure 13. Interface shear stress near the end of a broken fiber.

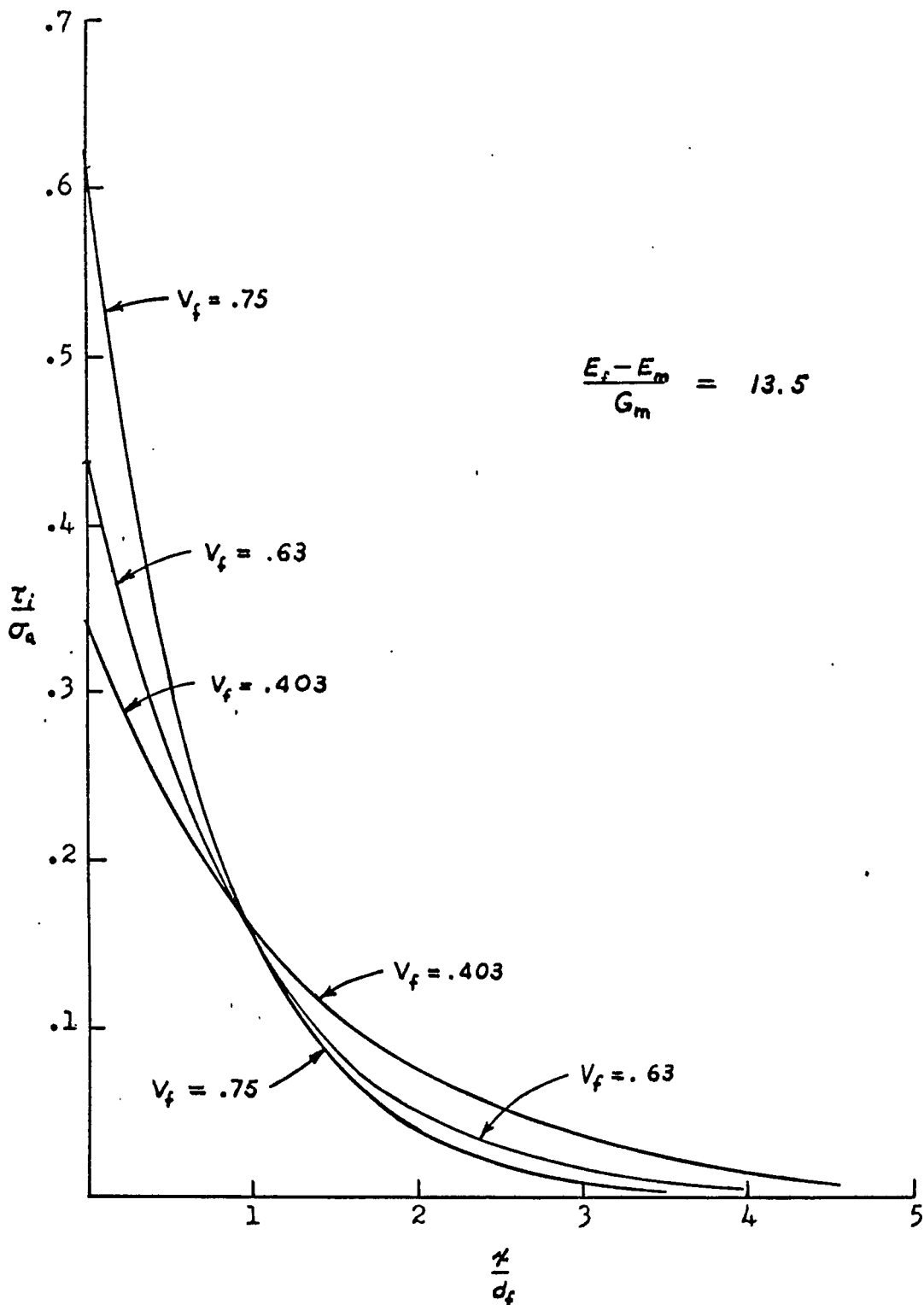


Figure 14. Interface shear stress near the end of a broken fiber.

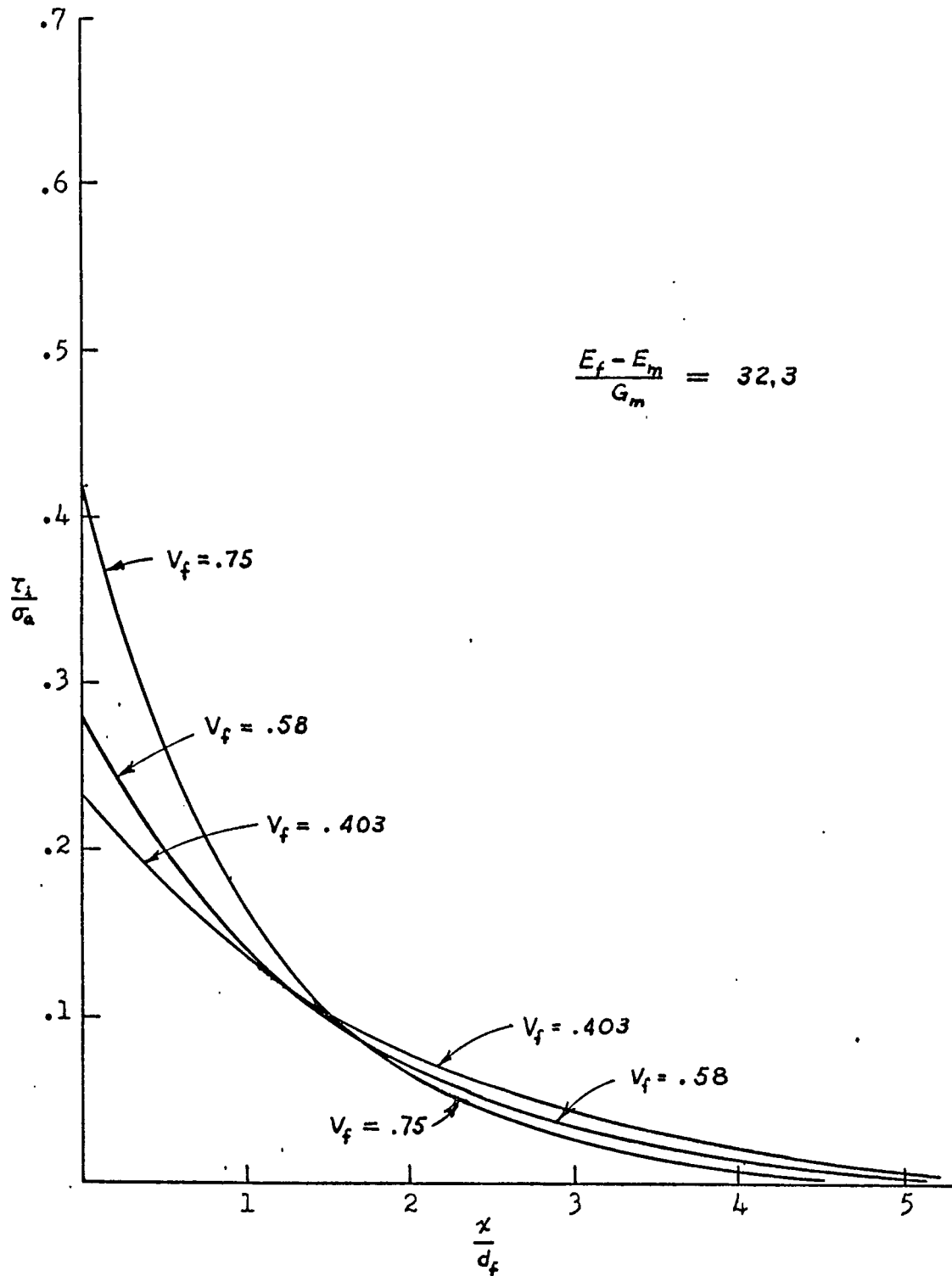


Figure 15. Interface shear stress near the end of a broken fiber.

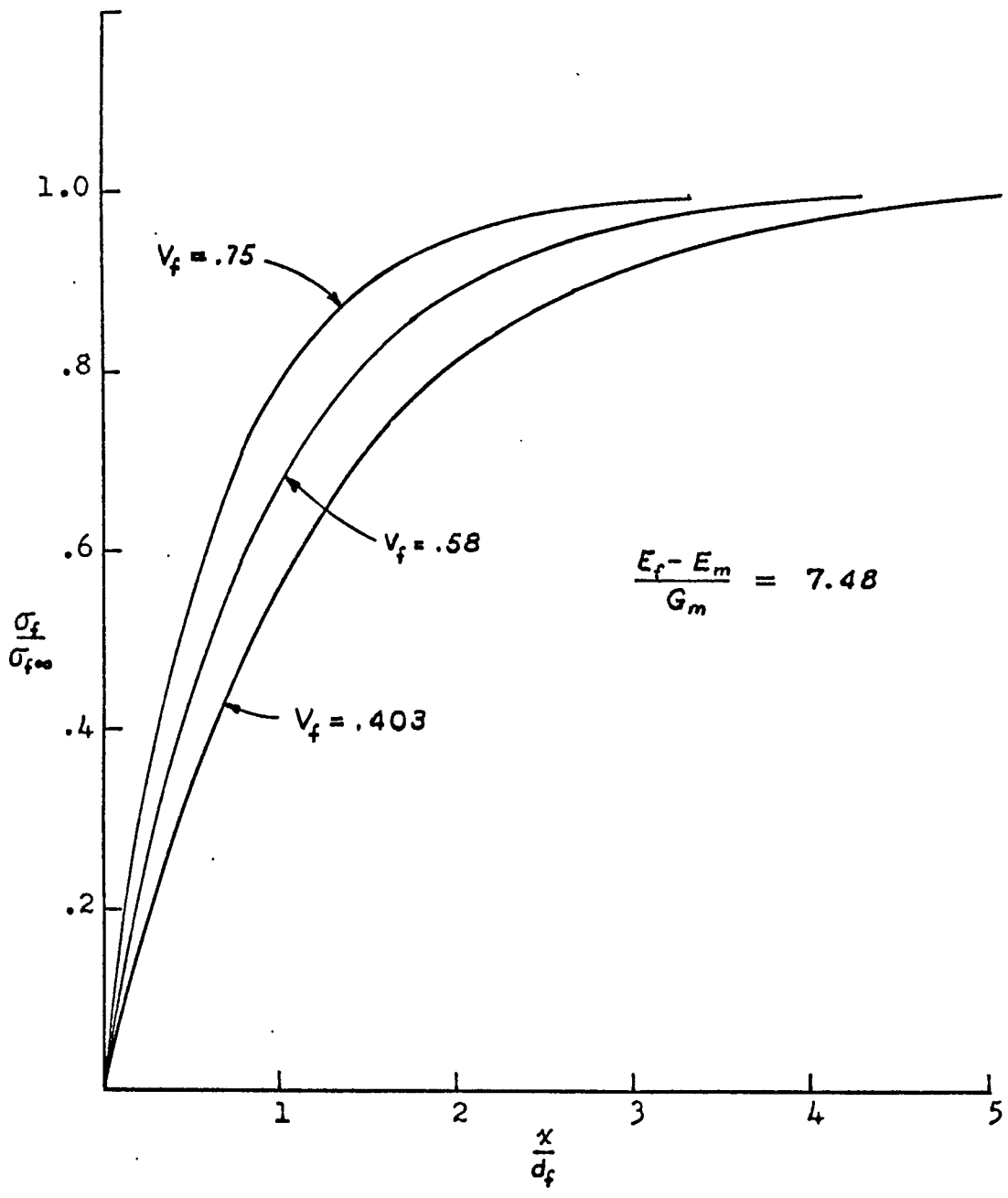


Figure 16. Distribution of tensile stress along a broken fiber.

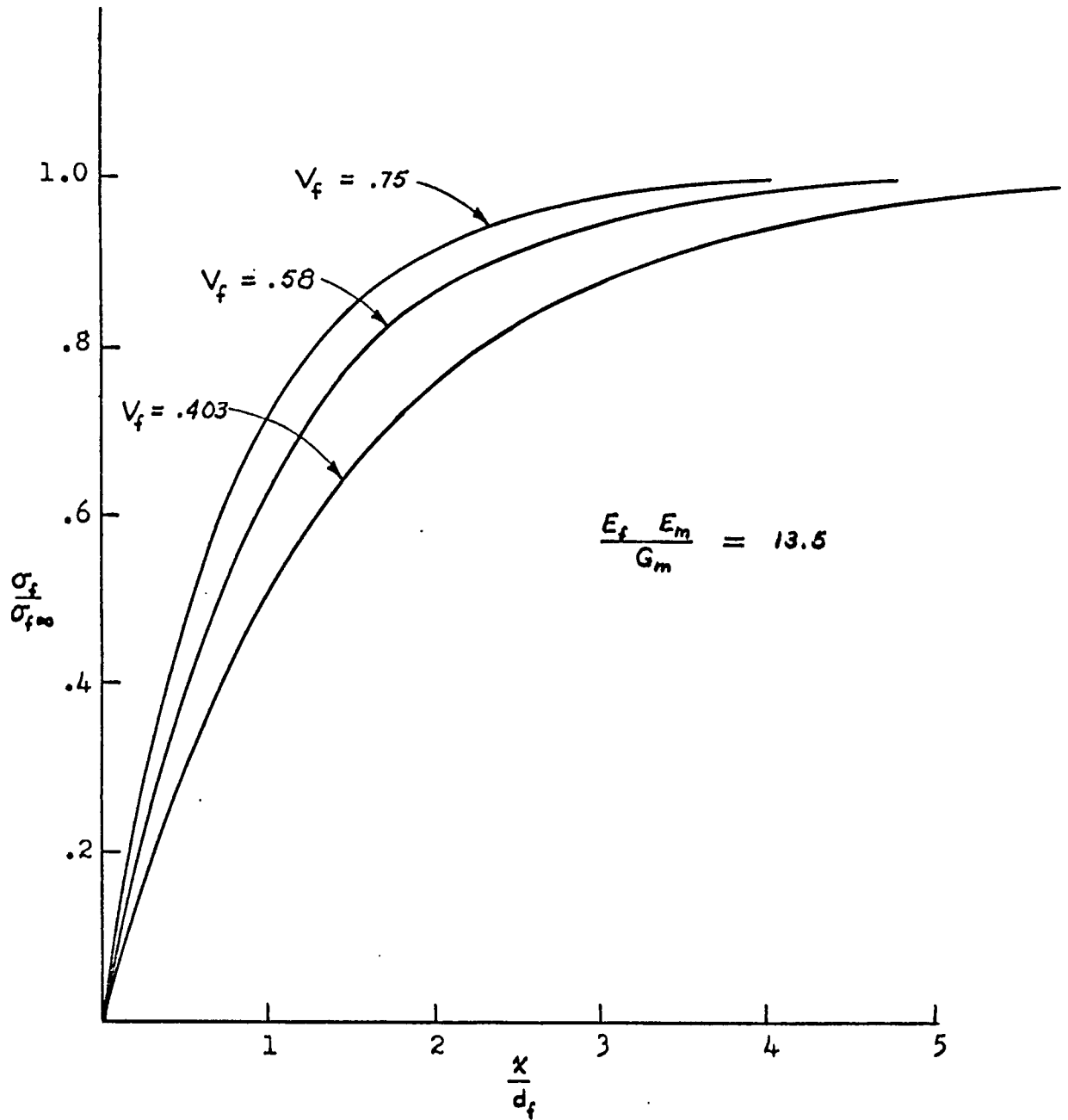


Figure 17. Distribution of tensile stress along a broken fiber.

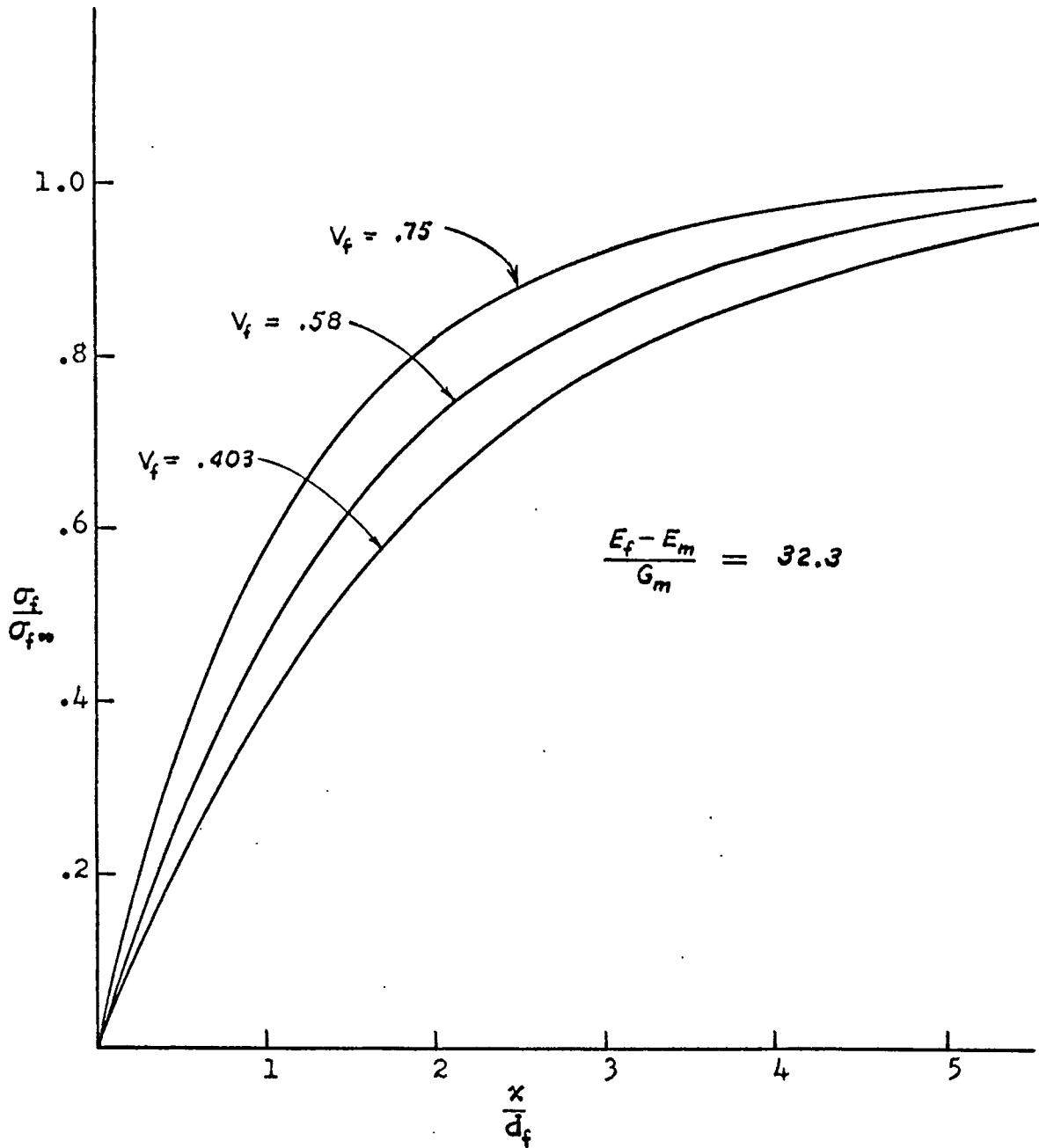


Figure 18. Distribution of tensile stress along a broken fiber.

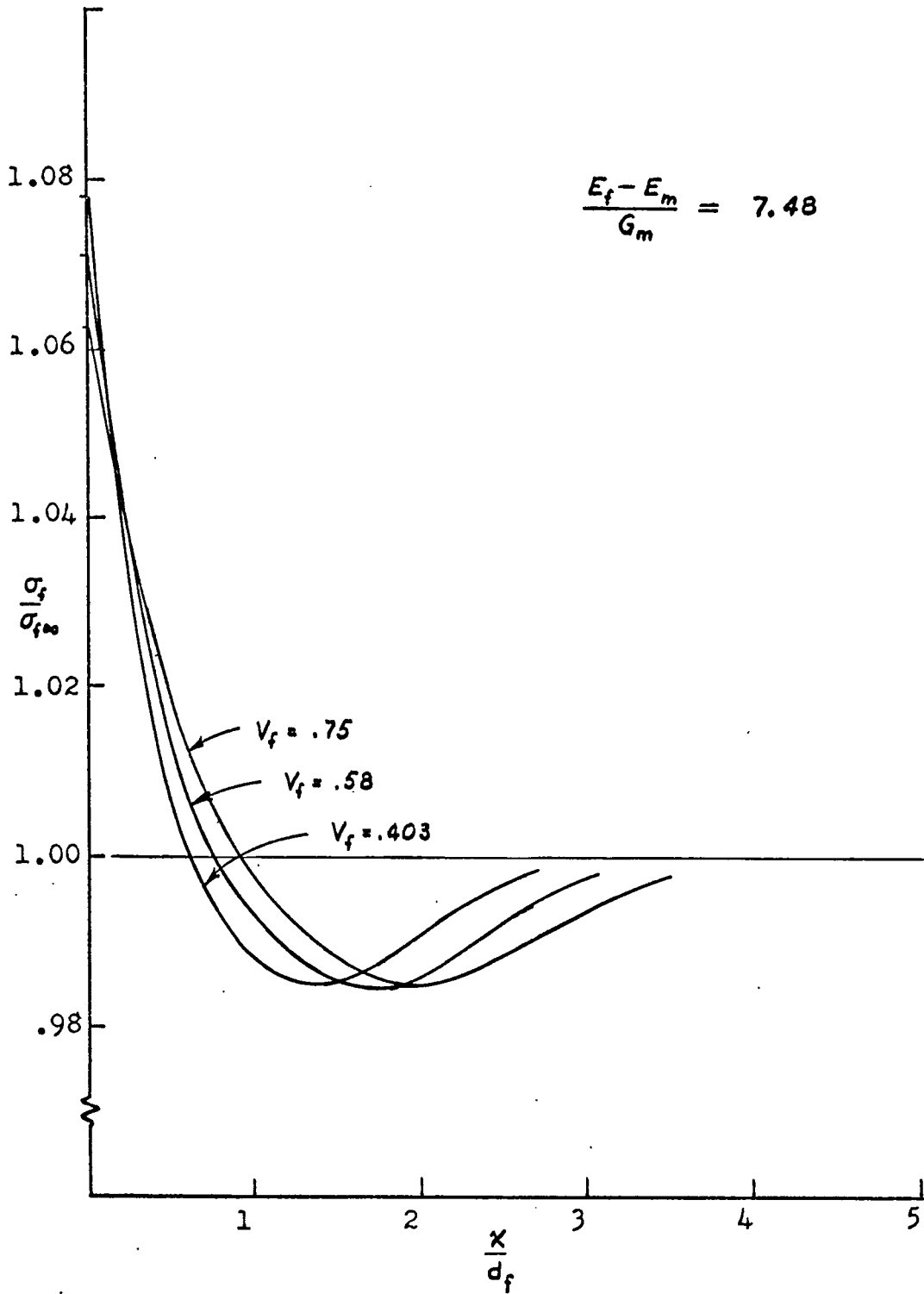


Figure 19. Perturbation of stress in fiber immediately adjacent to a fiber break.

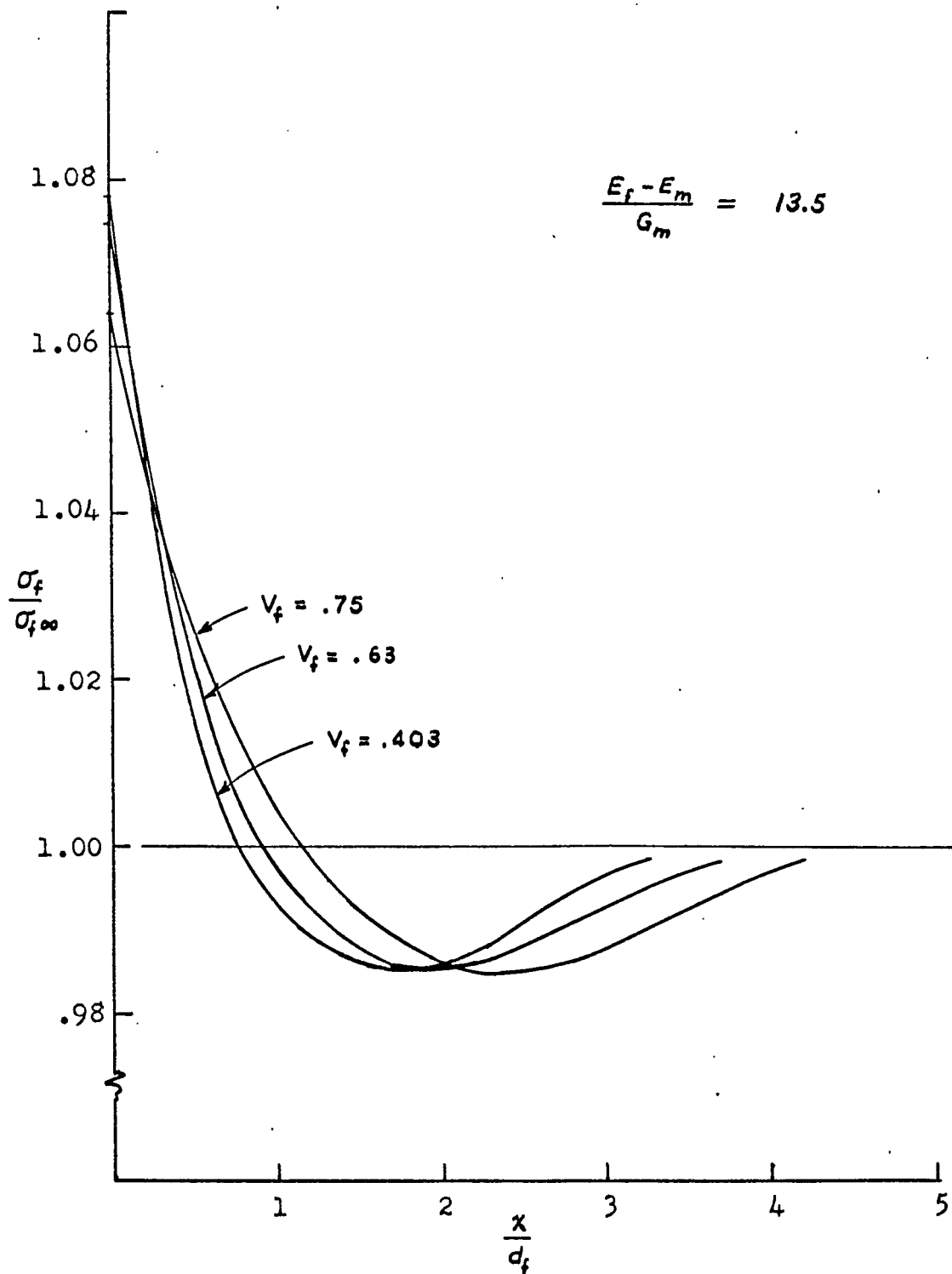


Figure 20. Perturbation of stress in fiber immediately adjacent to a fiber break.

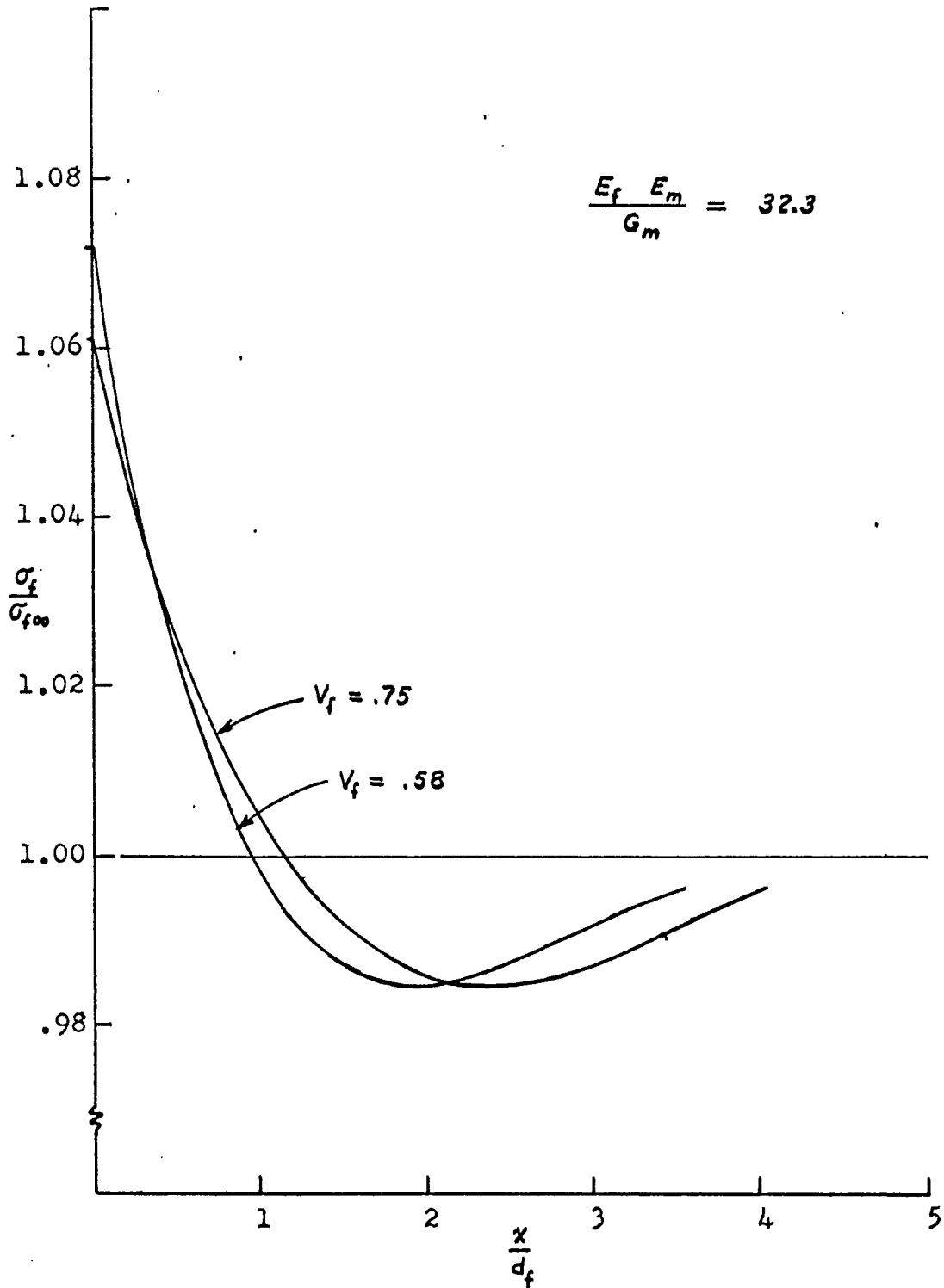


Figure 21. Perturbation of stress in fiber immediately adjacent to a fiber break.

CHAPTER IV

CONCLUSIONS

Although no claim of great precision can be offered for the results herein presented, they do indicate reasonable agreement with previous analyses of the same problem.

The discrete model and numerical analysis used in this study offers a distinct advantage in that it affords a means of evaluating stresses in the fibers adjacent to a broken fiber, while earlier analyses only deal with the stresses in and along the broken fiber itself.

The stress distribution in the fibers adjacent to a broken fiber is seen to be highly localized (Figures 19-21), the stress being raised within a zone less than one fiber diameter either side of the plane of the break. This, together with the fact that no stress disturbance is detected beyond the immediately adjacent fiber shows the localized nature of a fiber fracture in a reinforced composite, and leads to an explanation of the general toughness and lack of notch sensitivity found in fiber reinforced composite materials.

It has been shown that the breakage of a well bonded fiber results in only a small increase ($< 8\%$, Figures 19-21)

in stress over a length $\delta (< d_f)$ of the fibers immediately adjacent to the broken fiber. Over the remainder of the adjacent fiber ($x > \delta$), the fiber break produces a decrease in stress. Considering the small increment of stress, and the small region over which it acts, the probability that the stress increase will coincide with a flaw of sufficient magnitude to cause that fiber to break would be quite low for most fibers. The probability that a fracture will appear at some $x > \delta$ is essentially zero, since the stress has dropped there. The composite will, then, stabilize under the applied load. When the applied load is increased by some small amount, the probability of a break at some point far away from the initial break may be expected to be much greater than the probability that a break will appear in the vicinity of the initial break.

CHAPTER V

RECOMMENDATIONS FOR FURTHER RESEARCH

The results obtained in this study, when compared to previous theoretical results shows sufficient agreement to justify the model. As with any model of a physical system, however, application of the model must rest upon experimental evidence. Unfortunately, experimental values for stresses in a material of this type is lacking, since the only photoelastic evaluations available to date have been performed on isolated fibers. Attempts were made to extend the results of these experimental programs to the case of a discontinuous fiber in the near proximity of other fibers by making some approximations, but such extensions are themselves subject to question. This model, like those of Cox, Dow, and Rosen is sensitive to the method used to estimate mean distance between fibers, and more realistic results might be obtained if experimental results were available.

Photoelastic studies on a realistic model of the material treated here could be performed using stress freezing techniques. The application of such techniques would be tedious in terms of model preparation, which probably accounts for fact that it has not been done, but it is suggested that such an experimental program would be most beneficial at this time.

The model used herein might also be extended to a study of other packing configurations such as square or layered. Modifications could also be made to include bond failure in the model.

REFERENCES

1. Brenner, S.S., "Tensile Strength Of Whiskers," Jour. Appl. Phys., Vol. 27, No. 12 (Dec. 1956) pp. 1484-1191.
2. McDanel, D.L., R.W. Jech, and J.W. Weeton, "Metals Reinforced With Fibers," Metal Progress, Vol. 78, No.6 (Dec. 1960) pp. 118-121.
3. Kelly, A. and W.R. Tyson, "Tensile Properties Of Fibre-Reinforced Metals: Copper/Tungsten and Copper/Molybdenum," Jour. Mech. Phys. Solids, Vol. 13 (1965), pp. 329-350.
4. Cox, H.L., "The Elasticity And Strength Of Paper And Other Fibrous Materials," Brit. Jour. Appl. Phys., Vol. 3, No. 72 (Mar. 1952), pp. 72-79.
5. Outwater, J.O., Jr., "Plastics Reinforcement In Tension," Modern Plastics Vol. 33.2 (Mar. 1956), p. 156.
6. Levitt, A.B., "Whisker-Strengthened Metals," Mechanical Engineering, Vol. 89, No. 1 (Jan. 1967), pp. 36-42.
7. Rosen, B.W., N.F. Dow, and Z. Hashin, "Mechanical Properties Of Fibrous Composites," NASA Report CR-31, April 1964.
8. Cooper, G.A. and A. Kelly, "Tensile Properties Of Fibre-Reinforced Metals: Fracture Mechanics," Jour. Mech. Phys. Solids, Vol. 15 (1967), pp. 279-297.
9. Dow, N.F., Study Of Stresses Near A Discontinuity In A Filament-Reinforced Composite Metal G.E. Missile and Space Division Report R63SD61 Aug. 1963.
10. Tyson, W.R. and G.J. Davies, "A Photoelastic Study Of The Shear Stresses Associated With The Transfer Of Stress During Fibre Reinforcement." Brit. J. Appl. Phys. Vol. 16 (1965), pp. 199-205.
11. Schuster, D.M. and E. Scala, "The Mechanical Interaction Of Sapphire Whiskers With A Birefringent Matrix," Trans. Met. Soc. AIME, Vol. 230, pp. 1635-1640.

12. Scala, E., "Design And Performance Of Fibers And Composites" Fiber Composite Materials. Papers Presented At A Seminar Of The American Society For Metals, Oct. 17 and 18, 1964. American Society For Metals, Metals Park, Ohio, 1965, pp. 131-156.
13. Hollister, G.S. and C. Thomas, Fibre Reinforced Materials. Elsevier Publishing Co., Ltd., Barking, Essex, England, 1966.
14. Sutton, W.H. and J. Chorne, "Potential Of Oxide-Fiber Reinforced Metals," Fiber Composite Materials. Papers Presented At A Seminar Of The American Society For Metals, Oct. 17 and 18, 1964. American Society For Metals, Metals Park, Ohio, 1965, pp. 173-222.
15. Scarborough, James B., Numerical Mathematical Analysis, Johns Hopkins Press, Baltimore, Md., 1966, pp. 410-416.

APPENDIX I

MECHANICAL PROPERTIES OF FIBERS

Tables I and II contain selected representative values for some available reinforcing fibers. Values shown were compiled from Scala¹², Hollister and Thomas¹³ and Sutton and Chorne¹⁴.

TABLE I

THE PROPERTIES OF WHISKERS

Material	Ultimate Tensile Strength 10^6 psi.	Elastic Modulus E, 10^6 psi.	Specific Gravity, g	UTS/g 10^5 psi.	E/g 10^6 psi.	Melting Point °C
Graphite	2.8	98	2.2	12.7	45	3000
Al ₂ O ₃ whisker	2.2	60	4.0	5.5	15	2050
Al ₂ O ₃ large crystal	1.0	60	4.0	2.5	15	2050
BeO	2	59	3.0	6.7	20	2550
Si ₃ N ₄	2	55	3.1	6.5	18	1900
Fe	1.9	29	7.8	2.4	3.7	1540
SiC	1.6	70	3.2	5.0	2.2	2690
Cr	1.3	35	7.2	1.8	4.9	1890
Si	1.1	26	2.3	4.3	11	1450
B ₄ C	.96	66	2.5	3.8	26	2450
Ni	.56	31	9.0	.62	3.4	1455
Cu	.43	18	8.9	.48	2.0	1083

TABLE II

THE PROPERTIES OF CONTINUOUS FILAMENTS

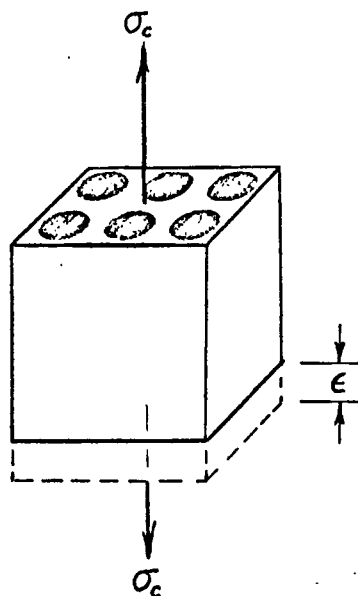
Material	Ultimate Tensile Strength 10 ⁶ psi.	Elastic Modulus E, 10 ⁶ psi.	Specific Gravity, g.	UTS/g 10 ⁵ psi.	E/g 10 ⁶ psi.	Melting Point °C
Asbestos (Crocidolite)	0.85	27	2.5	3.4	11	Loses water at 500
Mica	0.45	46	2.7	1.67	17	Loses water at 400
Etched Soda Glass	0.4 mean 0.5 max	9.8 9.8	2.5 2.5	1.6 2.0	3.9 3.9	
Drawn Silica (SiO ₂)	0.86	10.5	2.5	3.5	4.2	1660
E-Glass	0.25	10.5	2.5	1.0	4.2	840
Boron Glass	.35	64	2.3	1.5	27	
C	.18	6	1.9	.97	3.2	3700
W	.58	59	19	.30	3.1	3400
Mo	.32	52	10	.32	5.2	2622
Steel	.60	29	7.8	.77	3.7	
Be	.18	35	1.8	1.0	19.0	1284

APPENDIX II

LAW OF MIXTURES FOR CONTINUOUS FILAMENT REINFORCEMENT

When a composite contains reinforcing fibers which are continuous throughout the specimen, the fibers and the matrix are assumed to strain equally when a load is applied in the direction of the fibers.

Consider an element of composite of unit area and unit length subjected to an average composite stress σ_c . The element then undergoes a strain ϵ :



For a unit cross-section:

$$A_f + A_m = 1 \quad (\text{A2.1})$$

where A_f = Total cross sectional area of fibers

A_m = Total cross sectional area of matrix

Applying Hooke's Law to matrix and fibers:

$$\epsilon = \frac{\sigma_f}{E_f} = \frac{\sigma_m}{E_m} \quad (\text{A2.2})$$

The total load on the unit cross-section is:

$$\sigma_c = \sigma_f A_f + \sigma_m A_m \quad (\text{A2.3})$$

For this configuration, the area fraction is equal to the volume fraction:

$$A_f = V_f = \text{Fiber Volume Fraction} \quad (\text{A2.4})$$

Then, from (1):

$$A_m = 1 - V_f \quad (\text{A2.5})$$

Substituting (4) and (5) into (3):

$$\sigma_c = \sigma_f V_f + \sigma_m (1 - V_f) \quad (\text{A2.6})$$

Which is a Law of Mixtures for composite stress.

Then we may obtain a Composite Elastic Modulus by dividing (6) by ϵ :

$$\frac{\sigma_c}{\epsilon} = \frac{\sigma_f}{\epsilon} V_f + \frac{\sigma_m}{\epsilon} (1-V_f) \quad (\text{A2.7})$$

and applying Hooke's Law:

$$E_c = E_f V_f + E_m V_m \quad (\text{A2.8})$$

which is a Law of Mixtures formulation for the Composite Elastic Modulus in terms of the properties of the constituents.

APPENDIX III

THEORETICAL EVALUATIONS OF STRESS DISTRIBUTION IN AND AROUND
AN ELASTIC FIBER IN AN ELASTIC MATRIX WITH A STRONG BOND
STRESSED IN THE DIRECTION OF THE FIBER AXIS

Three theories have been offered. The models, assumptions, and derivations appear below in chronological order.

H. L. Cox⁴ (1952)

1. Assumptions:

- (a). The matrix is strained homogeneously, but the state of uniform stress and strain is locally perturbed by the transfer of load to the (more rigid) fiber.
- (b). Lateral stiffness of the fiber and matrix are equal.
- (c). Perfect bond exists between the fiber and the matrix at the lateral interface.
- (d). No load is transferred through the ends of the fiber.

2. Method: Cox assumed that the load is transferred from the matrix to the fiber according to the equation:

$$\frac{dP}{dx} = H(u-v) \quad (A3.1)$$

Where x = Distance from the fiber end
 P = Load carried by the fiber at x
 u = Displacement with fiber present
 v = Displacement of same point with fiber absent.
 H = A constant to be determined.

Equation (1) is Differentiated:

$$\frac{d^2P}{dx^2} = H\left(\frac{du}{dx} - \frac{dv}{dx}\right) \quad (A3.2)$$

Applying the Definition of Strain:

$$\frac{dv}{dx} = \text{Matrix Strain} = \epsilon \quad (A3.3)$$

$$\frac{du}{dx} = \text{Fiber Strain Difference} = \frac{P}{A_f E} \quad (A3.4)$$

Where $E = (E_f - E_m)$

Substituting (3) and (4) into (2):

$$\frac{d^2P}{dx^2} = H\left(\frac{P}{A_f E} - \epsilon\right) \quad (A3.5)$$

The Solution to Equation (5) is:

$$P = A_f E \epsilon + C_1 \cosh \beta x + C_2 \sinh \beta x \quad (A3.6)$$

Where $\beta^2 = \frac{H}{A_f E}$

Assuming the Boundary Conditions:

$$P = 0 \quad \text{at } x=0 \quad \text{and } x=l$$

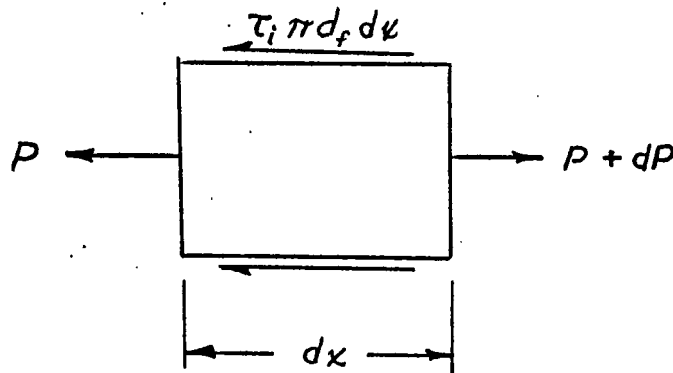
and Evaluating C_1 and C_2 , Equation (6) yields

$$P = A_f E \epsilon \left[1 - \frac{\cosh \beta \left(\frac{l}{2} - x \right)}{\cosh \beta \frac{l}{2}} \right] \quad (\text{A3.7})$$

Dividing by A_f , the fiber stress is obtained:

$$\sigma_f = (E_f - E_m) \frac{\sigma_a}{E_m} \left[1 - \frac{\cosh \beta \left(\frac{l}{2} - x \right)}{\cosh \beta \frac{l}{2}} \right] \quad (\text{A3.8})$$

Assuming that the fiber is of circular cross section, the interface shear τ_i may be related to the fiber load P by considering the Equilibrium of a Fiber Element:



Equilibrium Conditions Yield

$$\tau_i = \frac{1}{\pi d_f} \frac{dP}{dx} \quad (\text{A3.9})$$

or, Assuming that $P = \sigma_f A_f = \frac{\pi d_f^2}{4} \sigma_f$:

$$\tau_i = \frac{d_f}{4} \frac{d\sigma_f}{dx} \quad (\text{A3.10})$$

Differentiating (8) and Substituting it into (10):

$$\tau_i = \frac{(E_f - E_m) \sigma_a}{E_m} \frac{d_f}{4} \beta \frac{\sinh \beta (\frac{l}{2} - x)}{\cosh \beta \frac{l}{2}} \quad (\text{A3.11})$$

The Constant H for this Model is Defined as

$$H = \frac{2\pi G_m}{\ln \left(\frac{2r_o}{d_f} \right)} \quad (\text{A3.12})$$

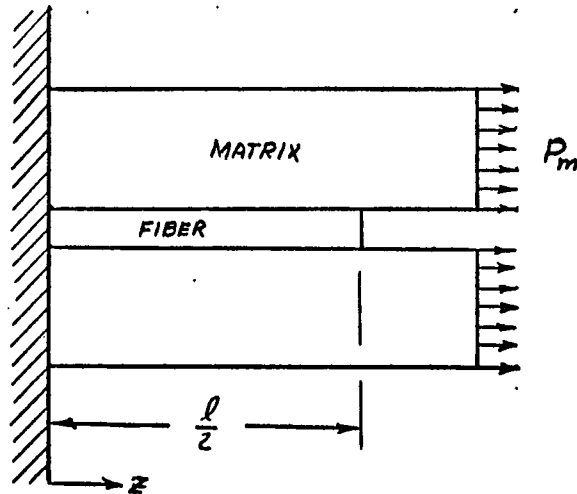
Where $r_o =$ Mean center distance between fibers.

N.F. Dow⁹ (1963)

1. Assumptions

- (a). No matrix at the end of the fiber, load is applied at one end to the matrix alone.
- (b). A perfect bond exists between fiber and matrix at the lateral interface.
- (c). Straight radial lines before deformation remain straight after deformation.

2. Method: The Model is shown below:



(a). Interface shear stress is obtained in terms of the change of force in the fiber and matrix as in Equation (A3.9).

$$\tau_i = -\frac{l}{\pi d_f} \frac{dF_f}{dz} \quad (\text{A3.13})$$

$$\tau_i = \frac{l}{\pi d_f} \frac{dF_m}{dz} \quad (\text{A3.14})$$

Where F_f and F_m are the forces in fiber and matrix, respectively. At $z=0$, there is no shear displacement, so

$$\frac{du_{\bar{r}_m}}{dz} = \frac{F_m}{A_m E_m} \quad (\text{A3.15})$$

$$\frac{du_{\bar{r}_f}}{dz} = \frac{F_f}{A_f E_f} \quad (\text{A3.16})$$

Where

\bar{r}_m = Distance of centroid of matrix from interface.

\bar{r}_f = Distance of centroid of fiber from interface.

u = Displacement in the z -Direction

(b). Shear strain in the fiber and matrix are given by:

$$\gamma_m = \frac{\tau_i}{G_m} = \frac{u_{\bar{r}_m} - u_i}{\bar{r}_m} \quad (\text{A3.17})$$

$$\gamma_f = \frac{\tau_i}{G_f} = \frac{u_i - u_{\bar{r}_f}}{\bar{r}_f} \quad (\text{A3.18})$$

Solving for u_i :

$$u_i = \frac{\frac{G_f}{\bar{r}_f} u_{\bar{r}_f} + \frac{G_m}{\bar{r}_m} u_{\bar{r}_m}}{\frac{G_f}{\bar{r}_f} + \frac{G_m}{\bar{r}_m}} \quad (\text{A3.19})$$

(c). Differentiating Equations (15) and (16) and Substituting into (13) and (14):

$$\tau_i = \frac{A_m E_m u_{\bar{r}_m}''}{\pi d_f} \quad (\text{A3.20})$$

$$\tau_i = \frac{A_f E_f u_{\bar{r}_f}''}{\pi d_f} \quad (\text{A3.21})$$

(d). Substituting Equations (20) and (21) into (17) and (18):

$$G_m \left[\frac{u_{\bar{r}_m} - u_i}{\bar{r}_m} \right] = \frac{A_m E_m u_{\bar{r}_m}''}{\pi d_f} \quad (\text{A3.22})$$

$$G_f \left[\frac{u_i - u_{\bar{r}_f}}{\bar{r}_f} \right] = \frac{A_f E_f u_{\bar{r}_f}''}{\pi d_f} \quad (\text{A3.23})$$

(e). Solving Equations (19), (22) and (23) yields:

$$(u_{\bar{r}_m}'' - u_{\bar{r}_f}'') - K^2 (u_{\bar{r}_m} - u_{\bar{r}_f}) = 0 \quad (\text{A3.24})$$

Where

$$K^2 = \pi d_f \left[\frac{\frac{G_m G_f}{\bar{r}_m \bar{r}_f}}{\frac{G_m}{\bar{r}_m} + \frac{G_f}{\bar{r}_f}} \right] \left[\frac{1}{A_m E_m} + \frac{1}{A_f E_f} \right] \quad (\text{A3.25})$$

the Solution of Equation, (24) is:

$$(u_{\bar{r}_m} - u_{\bar{r}_f}) = C_1 \cosh Kz + C_2 \sinh Kz \quad (\text{A3.26})$$

(f). The Boundary Conditions are

$$z = 0, \quad u_{\bar{r}_m} = u_{\bar{r}_f} = 0 \quad (\text{A3.27})$$

$$z = \frac{l}{2}, \quad \begin{cases} u'_{\bar{r}_m} = \frac{P_m}{A_m E_m} \\ u'_{\bar{r}_f} = 0 \end{cases} \quad (\text{A3.28})$$

hence,

$$C_1 = 0 \quad (\text{A3.29})$$

$$C_2 = \frac{P_m}{A_m E_m K \cosh K \frac{l}{2}} \quad (\text{A3.30})$$

then

$$(u_{\bar{r}_m} - u_{\bar{r}_f}) = \frac{P_m \sinh Kz}{A_m E_m K \cosh K \frac{l}{2}} \quad (\text{A3.31})$$

from Equations (20), (21), (22), (23), and (31):

$$\tau_i = \frac{P_m}{A_m E_m} \left[\frac{\frac{G_m G_f}{\bar{r}_m \bar{r}_f}}{\frac{G_m}{\bar{r}_m} + \frac{G_f}{\bar{r}_f}} \right] \frac{\sinh Kz}{K \cosh K \frac{l}{2}} \quad (\text{A3.32})$$

Defining

$$\lambda = K d_f \quad (\text{A3.24})$$

$$\text{and } z = \frac{l}{2} - x \quad (\text{A3.25})$$

Equation (32) becomes

$$\tau_z = \frac{\lambda P_m \sinh \frac{\lambda}{2d_f} (\frac{l}{2} - x)}{4 (A_f + \frac{A_m E_m}{E_f}) \cosh \frac{\lambda l}{2d_f}} \quad (\text{A3.25})$$

- (g). Substituting Equation (25) into (10) and solving:

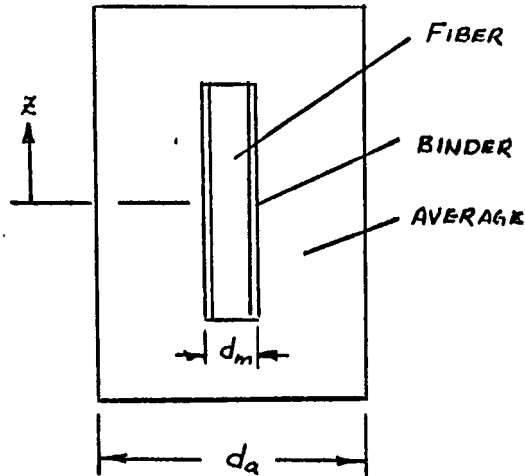
$$\sigma_f = \frac{P_m}{A_f + \frac{A_m E_m}{E_f}} \left[1 - \frac{\cosh \frac{\lambda}{2d_f} (\frac{l}{2} - x)}{\cosh \frac{\lambda l}{2d_f}} \right] \quad (\text{A3.26})$$

B.W. Rosen⁷ (1964)

1. Assumptions

- (a). Perfect bonding at the lateral interface.
- (b). No load transferred through the ends of the fiber.
- (c). Fiber and average material only carry tensile stresses.
- (d). Matrix only carries shear stresses.

2. Method: The model is shown below:



(a). The forces acting on an element of fiber are the same as in Dow's theory:

$$\tau_i = \frac{d_f}{4} \frac{d\sigma_f}{dz} \quad (\text{A3.27})$$

(b). For Equilibrium of the composite in the axial direction:

$$\left(\frac{d_f}{d_a}\right)^2 \sigma_f + \frac{(d_f^2 - d_a^2)}{d_a^2} \sigma_a = \sigma_c \quad (\text{A3.28})$$

Where

σ_a = Stress in the average material

σ_c = Applied stress

(c). The shear strain in the matrix is given by:

$$\gamma = \frac{u_a - u_f}{\frac{1}{2}(d_m - d_f)} \quad (\text{A3.29})$$

- (d). Differentiating Equation (29) twice and using Hooke's Law:

$$\frac{1}{E_a} \frac{d\sigma_a}{dz} - \frac{1}{E_f} \frac{d\sigma_f}{dz} = \frac{d_m - d_f}{4 G_m} \frac{d^2 \tau}{dz^2} \quad (\text{A3.30})$$

where E_a Modulus of average material

- (e). Differentiating Equation (28) and substituting the Results, with Equation (27) into Equation (30) yields:

$$\frac{d^2 \tau}{dz^2} - \eta^2 \tau = 0 \quad (\text{A3.31})$$

where

$$\eta^2 = \frac{8 G_m}{E_m (d_m - d_f) d_f} \left[1 + \frac{E_f}{E_a} \frac{d_f^2}{d_a^2 - d_m^2} \right] \quad (\text{A3.32})$$

The Solution of Equation (31) is

$$\tau = C_1 \sinh \eta z + C_2 \cosh \eta z \quad (\text{A3.33})$$

- (f). The Boundary Conditions are

$$\tau = 0 \quad \text{AT} \quad z = 0$$

$$\sigma_f = 0 \quad \text{AT} \quad z = \frac{l}{2}$$

from which

$$C_1 = \frac{2 G_m \sigma_c d_a^2}{\eta E_a (d_m - d_f) (d_a^2 - d_m^2) \cosh \eta \frac{l}{2}} \quad (\text{A3.34})$$

$$C_2 = 0$$

(g) Denoting $\kappa = \frac{l}{2} - x$, the expressions for τ_i and σ_f are:

$$\tau_i = \frac{2 G_m \sigma_c d_a^2 \sinh \eta \left(\frac{l}{2} - \kappa \right)}{\eta E_a (d_a - d_f) (d_a^2 - d_m^2) \cosh \eta \frac{l}{2}} \quad (\text{A3.35})$$

$$\sigma_f = \frac{\sigma_c d_a^2 E_f}{E_a (d_a^2 - d_m^2) + E_f d_f^2} \left[1 - \frac{\cosh \eta \left(\frac{l}{2} - \kappa \right)}{\cosh \eta \frac{l}{2}} \right] \quad (\text{A3.36})$$

APPENDIX IV

THE COMPUTER PROGRAM

COMPUTER FORTRAN STATEMENTS

```

DIMENSION SIGMAF(100,10),TAU(100,10), MESSAG(20)
REAL*8 U(100,10), SAVEF(100,10),F, FLOAD, BIGF, KT, KS
COMMON / RL / U, KT, KS, FLOAD, STRAT(12)
COMMON / INT / IMAX, JMAX
2 FORMAT (1H1, // 8X, 'TENSILE STRESSES IN FIBERS ' //)
3 FORMAT ( 8X, 4('SIGMAF(', I2, ', ', I2, ') = ', G13.6, 3X) )
4 FORMAT ( 8X, 4('TAU(', I2, ', ', I2, ') = ', G13.6, 6X) )
5 FORMAT (1H1, // 8X, 'RATIO OF LOCAL FIBER STRESS TO FIBER STRESS AT
1 INFINITY ' // 10X, 'Z/D', 3X, 4( 9X, 'FIBER(', I1, ') ' //)
6 FORMAT ( 8X, G13.6, (5( 4X, G13.6)))
7 FORMAT ( // 8X, 'TAU(0,1), EXTRAPOLATED ', G13.6, 10X, 'TAU(3,1), E
1 XTRAPOLATED ', G13.6)
8 FORMAT (1H1 // 10X, 'RATIO OF INTERFACE SHEAR STRESS TO APPLIED STRE
1 SS ' // 10X, 'Z/D', 10X, 'INTERFACE(1,2)', 10X, 'INTERFACE(2,3)' //)
9 FORMAT (5X, 3(5X, G13.6))
10 FORMAT (3E10.3, 4F10.4, 2I5)
11 FORMAT (1H1, // 10X, 10('*'), ' DATA ', 10('*') // 10X, 'FIBER ELASTIC MOD
1 ULUS = ', G15.8 // 10X,
2 'MATRIX FLASTIC MODULUS = ', G15.8 // 10X, 'MATRIX SHEAR MODULUS = '
3 G15.8 // 10X, 'FIBER DIAMETER = ', G13.6 // 10X, 'INCREMENT, DELTA Z =
4 ', G13.6 // 10X, 'DISTANCE BETWEEN FIBERS, T = ', G13.6 // 10X,
5 'AVERAGE OF APPLIED STRESS = ', G15.8 // 10X, 'IMAX = ', I3, 15X,
6 'JMAX = ', I3 // 10X, 40('*') //)
12 FORMAT ( 10X, 'FLOAD = ', G15.8, 3X, 'KT = ', G15.8, 3X, 'KS = ',
1 G15.8 // 10X, 'RATIO OF MINIMUM FIBER DISTANCE TO FIBER DIAMETER ',
2 G13.6 // 10X, 'VOLUME FRACTION = ', G13.6 // 1 X, 'RATIO OF ELASTIC MO
3 DULUS = ', G13.6, 'RATIO OF FIBER TENSILE MODULUS TO MATRIX SHEAR M
4 ODULUS = ', G13.6 //)
14 FORMAT (10X, 4('U(', I2, ', ', I2, ') = ', G13.6, 3X) )
16 FORMAT ( // 10X, 'EXIT ON SIZE OF RESIDUE AFTER ', I4, ' ITERATIONS, BIG
1 F = ', G15.6 //)
17 FORMAT (1H1, // 8X, 'SHEAR STRESSES IN MATRIX ' //)
19 FORMAT (1H1, // 10X, 'CORRECTED DISPLACEMENT FIELD ' //)
21 FORMAT ( // 10X, 'ESTIMATED ERROR = ', F5.3, ' PERCENT', //)
31 FORMAT ( // 10X, 'EXIT ON MAXIMUM NUMBER OF CORRECTIONS', 10X, 'BIGF
1 = ', G15.6 //)
33 FORMAT (20A4)
34 FORMAT ( // 10X, 10('*'), 20A4 //)
50 READ (5,10,FND=2000) EF, EM, GM, DIAF, DELTAZ, T, SIGAP, IMAX, JMAX
WRITE (6,11) EF, EM, GM, DIAF, DELTAZ, T, SIGAP, IMAX, JMAX
READ (5, 33) (MESSAG(I), I = 1, 20)
WRITE (6,34) (MESSAG(I), I = 1, 20)
AF = 3.14159*(DIAF**2)/4.
AC = ((DIAF + T)**2)*SQRT(3.)/2.
KT = (AF*(EF-FM) + AC*FM)/DELTAZ

```

```

FLOAD = SIGAP*AC
IF (T .LF. .732051*DIAF) TBAR = DIAF + T - .866025*DIAF*(ATAN((1.
1+ T/DIAF)/SQRT(3.-(1+T/DIAF)**2))/(1.+T/DIAF)+ SQRT(3. - (1.+
2 T/DIAF)**2)/3.)
IF (T .GF. .732051*DIAF) TBAR = DIAF+T-.7853982*SQRT(3.)*DIAF**2
1 /(DIAF+T)
KS = GM*(DIAF+T)*DELTAZ/(1.732051*TBAR)
VF = AF/AC
TDR = T/DIAF
FFFMR = FF/FM
FFGMR = FF/GM
WRITE (6, 12) FLOAD,KT,KS, TDR, VF, EFEMR, FFGMR
CALL COX (FF, EM, GM, DIAF, DELTAZ, TBAR, SIGAP, IMAX, VF)
KOUNT = 0
DO 150 J = JMAX, 12
150 STRAT (J) = 0.
DO 250 J = 1, JMAX
250 STRAT (J) = 1.
DO 200 I = 1, IMAX
DO 200 J=1,10
200 U(I,J) = FLOAD*(I-0.5)/KT
DO 300 I = 1, IMAX
DO 300 J = 1, JMAX
300 SAVEF(I,J) = F(I,J)
400 BIGF = 0.
KOUNT = KOUNT + 1
DO 500 I = 1, IMAX
DO 500 J = 1, JMAX
IF (DABS(SAVEF(I,J)) .LT. DABS(BIGF)) GO TO 500
BIGF = SAVEF(I,J)
IBIG = I
JBIG = J
500 CONTINUE
IF (DABS(BIGF) .GT. FLOAD/200.) GO TO 600
WRITE (6, 16) KOUNT, BIGF
GO TO 800
600 UTEMP = U(IBIG,JBIG)
FTEMP = F(IBIG,JBIG)
DFLU = 0.5*DELTAZ
U(IBIG,JBIG) = U(IBIG,JBIG) + DELU
DELF = F(IBIG,JBIG) - FTEMP
U(IBIG,J+IG) = UTEMP - FTEMP*DFLU/DELF
SAVEF(IBIG,JBIG) = F(IBIG,JBIG)
IF (IBIG .LT. IMAX) SAVEF(IBIG+1,JBIG) = F(IBIG+1,JBIG)
IF (IBIG .GT. 1) SAVEF(IBIG-1,JBIG) = F(IBIG-1,JBIG)
IF (JBIG .LT. JMAX) SAVEF(IBIG,JBIG+1) = F(IBIG,JBIG+1)
IF (JBIG .GT. 1) SAVEF(IBIG,JBIG-1) = F(IBIG,JBIG-1)
IF (KOUNT .LT. 1800) GO TO 400
WRITE (6, 31) BIGF

```

```

800 FRR = 100.*BIGF/FLOAD
   WRITE (6, 21) FRR
   WRITE (6, 19)
   DO 900 I = 1, IMAX
900  WRITE (6, 14) ( I, J, U(I,J), J=1,JMAX)
   DO 1100 J = 1, JMAX
   DO 1100 I = 1, IMAX
   IF (I .GT. 1) GO TO 1000
   IF (J .GT. 1) SIGMAF(I,J) = EF*2.*U(I,J)/DELTAZ
   IF (J .EQ. 1) SIGMAF(I,J) = 0.
   GO TO 1100
1000 SIGMAF(I,J) = EF*(U(I,J) - U(I-1,J))/DELTAZ
1100 TAU (I,J) = GM*(U(I,J) - U(I,J+1))/T
   WRITE (6, 2)
   DO 1200 I = 1, IMAX
1200 WRITE (6, 3) (I,J,SIGMAF(I,J), J=1,JMAX)
   WRITE (6, 17)
   DO 1300 I = 1, IMAX
1300 WRITE (6, 4) ( I,J,TAU(I,J), J= 1,JMAX)
   TAUEND = TAU(1,1)*SQRT(TAU(1,1)/TAU(2,1))
   CHK3 = ((TAU(2,1))**2)/TAU(1,1)
   WRITE (6, 7) TAUEND, CHK3
   WRITE (6, 5) (J, J = 1, JMAX)
   DO 1500 I = 1, IMAX
   ZR = (I-1)*DELTAZ/DIAF
   DO 1400 J = 1, JMAX
1400 SIGMAF(I,J) = SIGMAF(I,J)/SIGMAF(IMAX,JMAX)
1500 WRITE (6, 6) (ZR,(SIGMAF(I,J), J = 1, JMAX))
   WRITE (6, 8)
   DO 1700 I = 1, IMAX
   ZR = (I - 0.5)*DELTAZ/DIAF
   DO 1600 J = 1,2
1600 TAU(I,J) = TAU(I,J)/SIGAP
1700 WRITE (6,9) ZR, TAU(I,1), TAU(I,2)
   GO TO 50
2000 STOP
   FND

```

```

C . . . RESIDUE SUBROUTINE . . . . .
  REAL FUNCTION F*8(I,J)
  REAL*8 U(100,10), K, D, FTENSN, FSHEAR, FLOAD
  COMMON / RL / U, K, D, FLOAD, STRAT(12)
  COMMON / INT / IMAX, JMAX
  IUP = I + 1
  IRACK = I - 1
  JUP = J + 1
  JRACK = J - 1
  IF (I.NE.1.AND.I.NE.IMAX) FTENSN=K*(U(IUP,J)+U(IRACK,J) -2.*U(I,J))
  IF (I .EQ. IMAX) FTENSN = K*(U(IRACK,J)-U(I,J))+FLOAD
  IF (I .EQ. 1 .AND. J .NE. 1) FTENSN = K*(U(IUP,J)-3.*U(I,J))
  IF (I .EQ. 1 .AND. J .EQ. 1) FTENSN = K*(U(IUP,J)-U(I,J))
  IF (J .EQ. 1) GO TO 10
  IF (J .EQ. 2) GO TO 20
  IF (J .EQ. 3) GO TO 30
  IF (J .EQ. 4) GO TO 40
  WRITE (6, 3)
  3 FORMAT (// 10X,30('*'), 'ERROR ** J IS TOO LARGE', 30('*')/)
  GO TO 500
10 FSHEAR = 6.*D*(U(I,2)-U(I,1))
  GO TO 500
20 FSHEAR = D*(U(I,1)-U(I,2)+2.*STRAT(3)*(U(I,3)-U(I,2)) +
  1 STRAT(4)*(U(I,4) - U(I,2)))
  GO TO 500
30 FSHEAR = 2.*D*(U(I,2)-U(I,3)+STRAT(4)*(U(I,4)-U(I,3)) +
  1 STRAT(5)*(U(I,5) - U(I,3)))
  GO TO 500
40 FSHEAR = D*(U(I,2)+ 2.*U(I,3) - 3.*U(I,4) + 2.*STRAT(5)*(U(I,5)-
  1 U(I,4)) + STRAT(6)* (U(I,6) - U(I,4)))
500 CONTINUE
  F = FTENSN + FSHEAR
  RETURN
  END

```

```
SUBROUTINE COX(EF, FM, GM, DIAF, DELTAZ, T, SIGAP, IMAX, VF)
  BETA = SQRT(8.*GM/((EF-EM)*ALOG(1. + T/DIAF)))/DIAF
  FC = (EF-EM)*VF + EM
  K1 = SIGAP*FF/EC
  K1P = K1*BETA*DIAF/4.
  WRITE (6, 10)
10 FORMAT (1H1//20X, 'STRESSES ACTING ON CENTER FIBER ACCORDING TO COX
  1'// 25X, 'Z/D', 16X, 'SHEAR' 16X, 'TENSION'//)
  ILIMIT = IMAX+1
  DO 50 I = 1, ILIMIT
  Z = (I - 1) * DELTAZ
  ZR = Z/DIAF
  TAU = K1P*EXP(-BETA*Z)
  SIGMA = K1*(1. - EXP(-BETA*Z))
50 WRITE (6, 66) ZR, TAU, SIGMA
66 FORMAT ( 10X, 3(10X, G13.6))
  RETURN
  END
```